Synthesis of 2-aryl-1,2,4-oxadiazolo-benzimidazoles: Tubulin polymerization inhibitors and apoptosis inducing agents

ARTICLE *in* BIOORGANIC & MEDICINAL CHEMISTRY · JUNE 2015

Impact Factor: 2.79 · DOI: 10.1016/j.bmc.2015.05.060 · Source: PubMed

7 AUTHORS, INCLUDING:

Ahmed Kamal
Indian Institute of Chemical Technology
489 PUBLICATIONS **6,097** CITATIONS
SEE PROFILE

Srinivasa Reddy
RMIT University
16 PUBLICATIONS **38** CITATIONS
SEE PROFILE

Vijay Nimbarte
9 PUBLICATIONS **21** CITATIONS
SEE PROFILE

Srinivasulu Vunnam
South Korea
25 PUBLICATIONS **103** CITATIONS
SEE PROFILE

Bioorganic & Medicinal Chemistry xxx (2015) xxx–xxx

Contents lists available at ScienceDirect

Bioorganic & Medicinal Chemistry

journal homepage: www.elsevier.com/locate/bmc

Synthesis of 2-aryl-1,2,4-oxadiazolo-benzimidazoles: Tubulin polymerization inhibitors and apoptosis inducing agents

Ahmed Kamal [a,b,*], T. Srinivasa Reddy [a,b], M. V. P. S. Vishnuvardhan [a], Vijaykumar D. Nimbarte [a,b], A. V. Subba Rao [a], Vunnam Srinivasulu [a], Nagula Shankaraiah [b,*]

[a] Medicinal Chemistry and Pharmacology, CSIR-Indian Institute of Chemical Technology, Hyderabad 500 007, India
[b] Department of Medicinal Chemistry, National Institute of Pharmaceutical Education and Research (NIPER), Hyderabad 500 037, India

ARTICLE INFO

Article history:
Received 3 February 2015
Revised 29 May 2015
Accepted 30 May 2015
Available online xxxx

Keywords:
Benzimidazole
1,2,4-Oxadiazole
Cytotoxicity
Tubulin polymerization
Apoptosis
Molecular docking

ABSTRACT

A new series of 2-aryl 1,2,4-oxadiazolo-benzimidazole conjugates have been synthesized and evaluated for their antiproliferative activity in the sixty cancer cell line panel of the National Cancer Institute (NCI). Compounds **5l** (**NSC**: 761109/1) and **5x** (**NSC**: 761814/1) exhibited remarkable cytotoxic activity against most of the cancer cell lines in the one dose assay and were further screened at five dose concentrations (0.01, 0.1, 1, 10 and 100 μM) which showed GI_{50} values in the range of 0.79–28.2 μM. Flow cytometric data of these compounds showed increased cells in G2/M phase, which is suggestive of G2/M cell cycle arrest. Further, compounds **5l** and **5x** showed inhibition of tubulin polymerization and disruption of the formation of microtubules. These compounds induce apoptosis by DNA fragmentation and chromatin condensation as well as by mitochondrial membrane depolarization. In addition, structure activity relationship studies within the series are also discussed. Molecular docking studies of compounds **5l** and **5x** into the colchicine-binding site of the tubulin, revealed the possible mode of interaction by these compounds.

1. Introduction

Benzimidazoles have attracted significant interest in medicinal chemistry as they exhibit a broad range of biological activities such as antiulcer,[1] antimicrobial,[2] antioxidant,[3] antiviral,[4] anti-inflammatory[5] and anticancer activity.[6] For instance, Hoechst 33258 (**1**, Fig. 1),[7] nocodazole (**2**)[8] and bendamustin (**3**)[9] are some of the benzimidazole based anticancer drugs which are in clinical or preclinical studies. Benzimidazole substituted derivatives are also known inhibitors of tubulin polymerization that inhibit cell proliferation in the treatment of cancer.[8,9] Recently, we have reported the synthesis and anticancer activity of terphenyl benzimidazoles as tubulin polymerization inhibitors.[10] Among the benzimidazoles with anticancer potential, 2-aryl/heteroaryl benzimidazole based molecules exhibited pronounced activity, therefore design and synthesis of newer 2-aryl benzimidazoles is of much significance.[11,12]

Recently, there has been wide interest in compounds containing the 1,2,4-oxadiazole scaffold because of their wide range of biological activities such as antimicrobial,[13] antiviral,[14] anti-inflammatory[15] and antineoplastic.[16] Moreover, 1,2,4-oxadiazole heterocycles are widely used for the bioisosteric replacement of an ester or amide functionality with substantial improvement in biological activity by participating in hydrogen bonding interactions with different receptors.[17] Among the oxadiazoles, 3,5-disubstituted-1,2,4-oxadiazoles (**4**) are reported in the literature for their anticancer potential.[18]

On the basis of these observations and in continuation to our previous efforts aiming at finding promising new leads with potential anticancer activity, it was considered worthwhile to design and synthesize new hybrids that contain the 2-arylbenzimidazole as well as 1,2,4-oxadiazole ring systems. Furthermore, benzimidazole attached with other heterocyclic moieties resulted in compounds (hybrid molecules) with improved pharmacological profile.[19] Therefore, we have synthesized a series of new 2-arylbenzimidazole conjugates linked to the 1,2,4-oxadiazole moiety and evaluated for their cytotoxic activity at the National Cancer Institute (NCI), USA. Sixteen compounds were evaluated for their antiproliferative activity as per the NCI protocol and the results are shown in Table 2. In addition, cell cycle analysis and tubulin polymerization assay were carried out for the most potent compounds of the series (**5l** and **5x**) apart from the molecular docking study on the tubulin protein.

2. Chemistry

2-Arylbenzimidazole linked 1,2,4-oxadiazole conjugates **5a–x** were synthesized as shown in Scheme 1. The benzimidazole

* Corresponding authors. Tel.: +91 40 27193157; fax: +91 40 27193189 (A.K.), tel.: +91 40 23074750; fax: +91 040 23073751 (N.S.).
E-mail addresses: ahmedkamal@iict.res.in (A. Kamal), shankar@niperhyd.ac.in (N. Shankaraiah).

http://dx.doi.org/10.1016/j.bmc.2015.05.060
0968-0896/

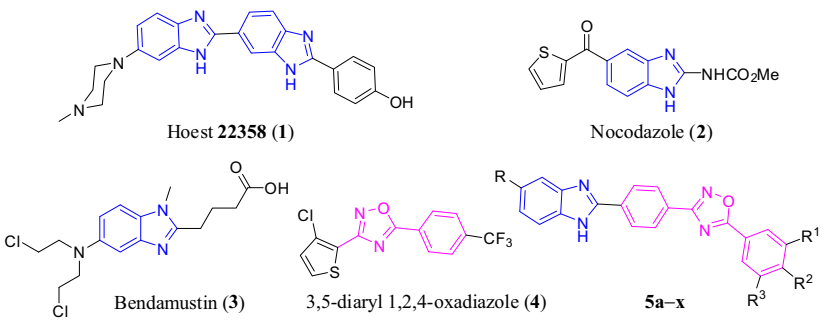

Figure 1. Chemical structures of Hoest 22358 (**1**), Nocodazole (**2**), Bendamustin (**3**), 3,5-diaryl 1,2,4-oxadiazole, and the newly synthesized molecules **5a–x**.

precursors 4-(1*H*-benzo[*d*]imidazol-2-yl)benzonitriles (**8a–d**) were synthesized by reacting 4-cyano benzaldehyde (**7**) with different substituted *o*-phenylenediamines (**6a–d**) in the presence of sodium metabisulfite, which were then reacted with hydroxylamine hydrochloride in ethanol under refluxing condition that resulted in the formation of corresponding amidoximes **9a–d**. The reaction of amidoximes **9a–d** with different aromatic carboxylic acids in the presence of carbonyl diimidazole (CDI) produced in situ *o*-acylamidoximes, which upon thermal cyclization afforded the desired target conjugates **5a–x** in good to moderate yields (39–68%).

3. Pharmacology

3.1. Anticancer activity

Primary screening of one-dose assay (10^{-5} M) was performed using a panel of about 60 human tumor cell lines which includes nine tumor subpanels namely; leukemia, non-small cell lung, colon, CNS, melanoma, ovarian, renal, prostate, and breast cancer cells, in accordance with the protocol of National Cancer Institute (NCI), USA. The compounds were added at a 10 μM concentration and the culture was incubated for 48 h. End point determinations were made with a protein binding dye, sulforhodamine B. Results for each compound were reported as a mean graph of the growth percent (GP) of the treated cells and the results obtained are illustrated in Table 1.

The results indicated a selective influence of some compounds on proliferation of a number of cancer cells with broad-spectrum of activity. Compound **5l** was highly active on leukemia cancer cell line (RPMI-8226) with GP = −15.28%, whereas compounds **5h**, **5x** and **5u** showed selective potency against ovarian cancer (OVACAR-4) cell line with GP = −8.43%, GP = −53.44, and GP = −21.59%, respectively. The majority of the tested compounds displayed growth inhibition on ovarian cancer cell line OVACAR-4 (**5h**, **5x**, **5t**, and **5u**) and different cell lines of leukemia (**5f**, **5j**, **5l**, **5s**). Close examination of the data presented in Table 1 indicated that marked growth inhibition was observed with the compounds **5l** and **5x** whereas **5f**, **5h**, and **5u** displayed moderate activity and all the remaining compounds were least active.

Among the tested compounds, **5l** and **5x** were further explored for the five dose assay at 10-fold dilutions of five different concentrations (0.01, 0.1, 1, 10 and 100 μM). Data of the five dose assay for compounds **5l** and **5x** is shown in Tables 2 and 3, respectively. The antiproliferative activity of tested compounds is given by three response parameters (GI_{50}, TGI and LC_{50}) for each cell line. The GI_{50} value (growth inhibitory activity) corresponds to the concentration of the compound that inhibits 50% net cell growth; the TGI value (cytostatic activity) is the concentration of the compound leading to total growth inhibition and the LC_{50} value (cytotoxic activity) is the concentration of the compound causing 50% net cell death at the end of the incubation period of 48 h. Furthermore, a mean graph midpoint (MG-MID) value is calculated giving an averaged activity parameter for all the cell lines.

Compound **5l** under investigation exhibited potent anticancer activity against all the tested cancer cell lines representing nine different subpanels with GI_{50} values between 1.30–8.27 μM

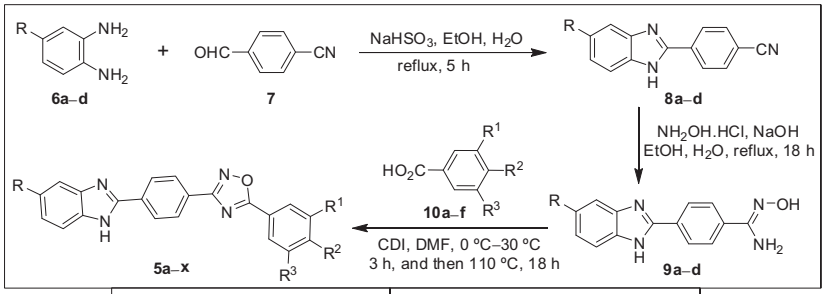

5a; R = R^1 = R^2 = R^3 = H	**5m**; R = Cl, R^1 = R^2 = R^3 = H
5b; R = R^1 = H, R^2 = F, R^3 = H	**5n**; R = Cl, R^1 = H, R^2 = F, R^3 = H
5c; R = R^1 = H, R^2 = Cl, R^3 = H	**5o**; R = Cl, R^1 = H, R^2 = Cl, R^3 = H
5d; R = R^1 = H, R^2 = OMe, R^3 = H	**5p**; R = Cl, R^1 = H, R^2 = OMe, R^3 = H
5e; R = R^1 = H, R^2 = Me, R^3 = H	**5q**; R = Cl, R^1 = H, R^2 = Me, R^3 = H
5f; R = H, R^1 = R^2 = R^3 = OMe	**5r**; R = Cl, R^1 = R^2 = R^3 = OMe
5g; R = F, R^1 = R^2 = R^3 = H	**5s**; R = OMe, R^1 = R^2 = R^3 = H
5h; R = F, R^1 = H, R^2 = F, R^3 = H	**5t**; R = OMe, R^1 = H, R^2 = F, R^3 = H
5i; R = F, R^1 = H, R^2 = Cl, R^3 = H	**5u**; R = OMe, R^1 = H, R^2 = Cl, R^3 = H
5j; R = F, R^1 = H, R^2 = OMe, R^3 = H	**5v**; R = OMe, R^1 = H, R^2 = OMe, R^3 = H
5k; R = F, R^1 = H, R^2 = Me, R^3 = H	**5w**; R = OMe, R^1 = H, R^2 = Me, R^3 = H
5l; R = F, R^1 = R^2 = R^3 = OMe	**5x**; R = R^1 = R^2 = R^3 = OMe

Scheme 1. Synthetic strategy for the generation of a library of novel 2-aryl 1,2,4-oxadiazolo-benzimidazole conjugates **5a–x**.

Table 1
Range and mean growth % of NCI cancer cell lines treated with selected compounds at 10 μM

Compound	NSC code	Mean growth	Range of growth	Most sensitive cell line	Growth % of most sensitive cell line
5b	**NSC**: 761111/1	98.97	81.29–113.60	K-562 (Leukemia)	81.29
5c	**NSC**: 761112/1	99.24	82.31–122.33	PC-3 (Prostate)	82.31
5f	**NSC**: 761108/1	74.72	28.37–115.83	CCRF-CEM (Leukemia)	28.37
5h	**NSC**: 761110/1	73.57	−8.43 to 118.66	OVCAR-4 (Ovarian Cancer)	−8.43
5i	**NSC**: 761843/1	103.42	81.02–114.94	A-498 (Renal Cancer)	81.02
5j	**NSC**: 761125/1	98.44	70.51–124.80	HL-60(TB) (Leukemia)	70.51
5k	**NSC**: 761124/1	97.66	81.24–141.54	OVCAR-4 (Ovarian Cancer)	81.24
5l	**NSC**: 761109/1	38.78	−15.28 to 81.52	RPMI-8226 (Leukemia)	−15.28
5r	**NSC**: 761815/1	99.09	81.15–121.55	HOP-92 (Non-Small Cell Lung Cancer)	81.15
5s	**NSC**: 761842/1	100.26	70.27–117.35	SR (Leukemia)	70.27
5t	**NSC**: 761136/1	89.70	45.60–114.98	OVCAR-4 (Ovarian Cancer)	45.60
5u	**NSC**: 761135/1	71.59	−21.59 to 120.05	OVCAR-4 (Ovarian Cancer)	−21.59
5v	**NSC**: 761828/1	101.65	79.71–122.24	A-498 (Renal Cancer)	79.71
5w	**NSC**: 761829/1	97.71	68.52–122.47	MCF-7 (Breast Cancer	68.52
5x	**NSC**: 761814/1	62.63	−53.44 to 115.73	OVCAR-4 (Ovarian Cancer)	−53.44

(Table 2). With regard to the sensitivity of the compound **5l** against individual cell line, the highest growth inhibitory activity was observed against the NCI-H322M cell line of non-small cell lung cancer with GI_{50} value 1.30 μM and minimum growth inhibitory activity against TK-10 cell line of renal cancer with GI_{50} value 8.27 μM. The compound **5x** also showed potent and highest growth inhibitory activity against BT-549 (breast cancer) cell line with GI_{50} value of 0.52 μM, SR (leukemia) cell line with GI_{50} value of 0.71 μM and least activity on A-498 (renal) cell line with GI_{50} value of 28.2 μM (Table 3). Moreover, compound **5x** is selectively sensitive towards all the leukemia cancer cell lines with GI_{50} values not more than 6.02 μM concentrations. The remaining subpanel cell lines showed maximum sensitivity towards these compounds with not more than 28 μM concentration. Overall, the screening process resulted in GI_{50} values of less than 28.2 μM indicating an exceptional activity and the values of LC_{50} are >100 μM in most of the cell lines, which indicates that these compounds are selectively toxic to cancer cells.

The criterion for selectivity of the compound towards a cancer cell line is based on the ratio obtained by dividing the full panel MG-MID (the average sensitivity of all cell lines towards the test agent) of the compounds by their individual subpanel MG-MID (the average sensitivity of all cell lines of a particular subpanel towards the test agent). Ratios between 3 and 6 refer to moderate selectivity, ratios greater than 6 indicate high selectivity toward the corresponding cell line, while compounds not meeting either of these criteria are rated non-selective.[20] As per this criterion, **5x** appears to be moderately selective towards leukemia cancer subpanel with selective index of 3.46 and **5l** was found to be non-selective with broad spectrum of antitumor activity against the nine tumor subpanels with selectivity ratios ranging between 0.74 and 1.35 at the GI_{50} levels.

Structure activity relationship was established based on the number of cell lines that showed sensitivity towards each of the newly synthesized compounds. Among all conjugates, the compounds **5f**, **5l**, and **5x** having methoxy groups at R^1, R^2, and R^3 positions have shown better antiproliferative activity. The activity was also influenced by the presence of weak ring de-activating groups like fluorine and electron releasing groups like methoxy at R substitution of benzimidazole ring. For instance, compounds **5h** and **5l** having fluoro group showed increased sensitivity on OVCAR-4 (ovarian cancer) cell line (−8.43% at 10 μM) and RPMI-8226 (leukemia) cell line (−15.28% at 10 μM) when compared to the unsubstituted derivatives. Furthermore, the presence of electron withdrawing groups like chloro (**5r**) on benzimidazole ring resulted in a dramatic loss of growth inhibitory effect. In view of the promising antiproliferative activity and higher therapeutic ratio of the compounds **5l** and **5x**, it was considered of interest to understand the detailed biological implicating by these compounds.

3.2. Effect on cell cycle arrest

To investigate the mechanism underlying the antiproliferative effect of these conjugates **5l** and **5x**, we examined the effect of these compounds on cell cycle progression by flow-cytometry in MCF-7 cells and nocodazole was used as a positive control. In this study, MCF-7 cells were treated with the compounds **5l** and **5x** at concentrations of 1 μm and 3 μm for a period of 48 h. Cells were harvested and the percentage of cells in each phase were analyzed by flow cytometry. The results are shown in Figures 2A and 2B. The data obtained clearly indicated that, these compounds arrest the cells in G2/M phase of the cell cycle in comparison to control. It was found that a large proportion of cells treated with the conjugates **5l** and **5x** accumulated in the G2/M phase, that is, 35.83% at 1 μM, 44.01 at 3 μM and 38.94% at 1 μM, 52.15 at 3 μM, respectively.

3.3. Effect on tubulin polymerization

Tubulin polymerization dynamics within the cells are critical for completion of mitosis and frequently targeted by agents that induce mitotic arrest by interfering with the mitotic spindle formation.[20] If the function of microtubules is blocked, cell differentiation will be arrested which leads to the accumulation of cells at G2/M phase in cell cycle analysis and it eventually leads to cell death.[21] Therefore, the two potent compounds in the series **5l** and **5x**, which induced cell cycle arrest at G2/M phase were evaluated for their effects on tubulin polymerization along with the positive control, nocodazole. The 3-(4-(1*H*-benzo[*d*]imidazol-2-yl)phenyl)-5-phenyl-1,2,4-oxadiazole conjugates (**5l**, **5x**) and nocodazole were employed at a concentration of 3 μm in tubulin assembly assays. The compounds **5l** and **5x** have exhibited potent inhibition of microtubule assembly with 55.6% and 52.1% inhibition, respectively, these values are comparable to that of standard nocodazole. Furthermore, the IC_{50} values of these conjugates were determined for their ability to inhibit tubulin assembly and the two lead molecules **5l** and **5x** showed pronounced inhibition of tubulin polymerization with IC_{50} values of 1.5 μM and 1.8 μM, respectively, as compared with 1.7 μM for nocodazole (Table 4). Overall, these results suggest that the compounds **5l** and **5x** significantly inhibit the tubulin polymerization.

Please cite this article in press as: Kamal, A.; et al. *Bioorg. Med. Chem.* (2015), http://dx.doi.org/10.1016/j.bmc.2015.05.060

Table 2
Cytotoxicity of **5l** (NSC 742530) against a panel of 60 human cancer cell lines

Cancer type	Cell line	GI_{50} (μM)	Subpanel MID	MGMID	TGI_{50} (μM)	LC_{50} (μM)
Leukemia	CCRF-CEM	2.97			>100	>100
	HL-60(TB)	2.24	2.42	1.34	>100	>100
	MOLT-4	1.99			>100	>100
	RPMI-8226	1.94			>100	>100
	SR	2.98			>100	>100
Non-small cell lung cancer	A549/ATCC	3.42			>100	75.6
	EKVX	3.45			>100	>100
	HOP-62	3.21	2.70	1.2	>100	53.6
	HOP-92	1.76			19.9	>100
	NCI-H226	2.72			>100	34.3
	NCI-H23	2.50			36.4	>100
	NCI-H322M	1.30			>100	>100
	NCI-H460	2.97			20.1	>100
	NCI-H522	3.04			16.9	51.6
Colon cancer	COLO 205	4.77			30.8	43.6
	HCC-2998	6.13			42.5	>100
	HCT-116	2.13	3.79	0.85	>100	>100
	HCT-15	3.15			>100	>100
	HT29	3.69			83.5	41.2
	KM12	3.08			18.0	>100
	SW-620	3.61			>100	>100
CNS cancer	SF-268	3.99			81.6	56.7
	SF-295	2.31			35.6	>100
	SF-539	3.37	4.33	0.75	60.8	>100
	SNB-19	5.62			>100	>100
	SNB-75	7.74			20.5	>100
	U251	3.03			>100	8.45
Melanoma	LOX IMVI	1.65			46.4	28.8
	MALME-3M	2.32			17.2	36.0
	M14	3.23	2.91	1.11	55.5	42.3
	MDA-MB-435	2.73			3.71	60.5
	SK-MEL-2	4.21			>100	56.4
	SK-MEL-28	3.78			79.0	34.0
	SK-MEL-5	2.22			>100	48.8
	UACC-257	3.70			>100	41.4
	UACC-62	2.35			>100	90.1
Ovarian cancer	IGROV1	3.81			62.7	>100
	OVCAR-3	2.56			6.98	56.5
	OVCAR-4	2.82	3.39	0.95	78.2	>100
	OVCAR-5	5.59			>100	72.4
	OVCAR-8	2.36			>100	>100
	NCI/ADR-RES	2.49			>100	>100
	SK-OV-3	4.12			80.5	>100
Renal cancer	786-0	3.61			61.7	>100
	A498	4.19			10.5	68.8
	ACHN	3.72			>100	>100
	CAKI-1	2.76	3.81	0.85	>100	>100
	RXF 393	1.90			58.6	>100
	SN12C	3.59			>100	>100
	TK-10	8.27			>100	>100
	UO-31	2.51			>100	22.8
Prostate cancer	PC-3	2.33	3.14	1.03	>100	>100
	DU-145	3.96			53.5	>100
Breast cancer	MCF7	2.88			>100	80.2
	MDA-MB-231/ ATCC	2.39			86.8	>100
	HS 578T	2.27	2.79	1.16	31.7	>100
	BT-549	3.49			>100	8.23
	T-47D	2.72			>100	>100
	MDA-MB-468	3.01			6.97	>100
MID[a]	60	3.25				

[a] Mean inhibitory dose.

3.4. Immunohistochemistry (IHC) of tubulin

In order to substantiate the observed cytotoxic effects of these compounds on the inhibition of tubulin polymerization to functional microtubules, immunohistochemistry studies have been carried out to examine the in situ effects of compounds **5l** and **5x** on cellular microtubules. Therefore, MCF-7 cells were treated with **5l** and **5x** at 1 μM concentration for 48 h. In this study, untreated human breast cancer cells displayed the normal distribution of microtubules. However, cells treated with **5l** and **5x** showed disrupted microtubule organization as seen in Figure 3, thereby demonstrating the inhibition of tubulin polymerization. This

Table 3
Cytotoxicity of **5x** against a panel of 60 human cancer cell lines

Cancer type	Cell line	GI_{50} (μM)	Subpanel MID	MGMID	TGI_{50} (μM)	LC_{50} (μM)
Leukemia	CCRF-CEM	2.20			>100	>100
	HL-60(TB)	2.02	2.90	3.46	81.7	>100
	K-562	1.20			>100	>100
	MOLT-4	5.29			59.1	>100
	RPMI-8226	6.02			>100	>100
	SR	0.71			>100	>100
Non-small cell lung cancer	A549/ATCC	5.65			20.5	55.5
	EKVX	26.2			84.9	>100
	HOP-62	4.44	11.11	0.90	16.8	47.1
	HOP-92	14.3			33.5	78.5
	NCI-H226	22.7			81.4	>100
	NCI-H23	4.10			20	57.8
	NCI-H460	4.60			22.5	90.9
	NCI-H522	6.89			45.3	>100
Colon cancer	HCC-2998	35.5			>100	>100
	HCT-116	1.90			10.7	40.7
	HCT-15	1.49	9.16	1.09	13.3	82.9
	HT29	2.70			15.2	>100
	KM12	7.52			81.8	>100
	SW-620	5.89			56.5	>100
CNS cancer	SF-268	7.13			45.6	>100
	SF-295	15.0			38.3	98.0
	SF-539	2.00	8.50	1.18	3.83	7.32
	SNB-19	12.7			36.8	>100
	SNB-75	12.5			27.4	60.1
	U251	1.68			4.88	17.7
Melanoma	LOX IMVI	13.3			34.6	90.2
	MALME-3M	1.67			7.51	>100
	M14	5.47	9.72	1.03	22.7	78.3
	MDA-MB-435	4.27			39.8	>100
	SK-MEL-2	18.9			51.1	>100
	SK-MEL-28	9.59			27.0	74.1
	SK-MEL-5	3.25			17.3	44.0
	UACC-257	17.1			46.9	>100
	UACC-62	14.0			33.4	79.6
Ovarian cancer	IGROV1	26.3			69.1	>100
	OVCAR-3	4.25			12.9	38.3
	OVCAR-4	1.88	11.81	0.85	4.79	16.5
	OVCAR-5	16.7			53.8	>100
	OVCAR-8	4.93			26.4	>100
	NCI/ADR-RES	3.32			23.6	>100
	SK-OV-3	25.3			64.8	>100
Renal cancer	A498	28.0			>100	>100
	ACHN	28.2			>100	>100
	CAKI-1	23.4			54.9	>100
	RXF 393	5.24	17.3	0.58	19.1	>100
	SN12C	13.2			31.3	46.5
	TK-10	4.62			13.0	74.2
	UO-31	18.9			38.7	43.1
Prostate cancer	PC-3	20.5	14.99	0.67	>100	79.2
	DU-145	9.48			28.3	>100
Breast cancer	MCF7	1.08			22.1	81.9
	MDA-MB-231/	2.65			13.9	>100
	ATCC				55.7	40.2
	HS 578T	9.49	4.99	2.01	2.11	>100
	BT-549	0.52			35.9	
	T-47D	14.7			26.3	87.4
	MDA-MB-468	6.54				85.3
MID[a]	60	10.05				

[a] Mean inhibitory dose.

immunofluorescence study showed that the level of tubulin polymerization inhibition was comparable to that of nocodazole for these conjugates (**5l** and **5x**).

3.5. Competitive colchicine binding assay

As the compounds **5l** and **5x** showed significant inhibitory effects on the tubulin polymerization, we investigated their mode of binding to the tubulin by fluorescence based assay.[22] The results from the Figure 4 indicated that that the compound **5x** as well as nocodazole showed significant affinity towards the colchicine site on the tubulin, whereas **5l** showed moderate or low binding affinity in comparison to nocodazole. Moreover, taxol was used as a negative control, which is known to bind at a different site and shows no effect on tubulin–colchicine complex.

Please cite this article in press as: Kamal, A.; et al. *Bioorg. Med. Chem.* (2015), http://dx.doi.org/10.1016/j.bmc.2015.05.060

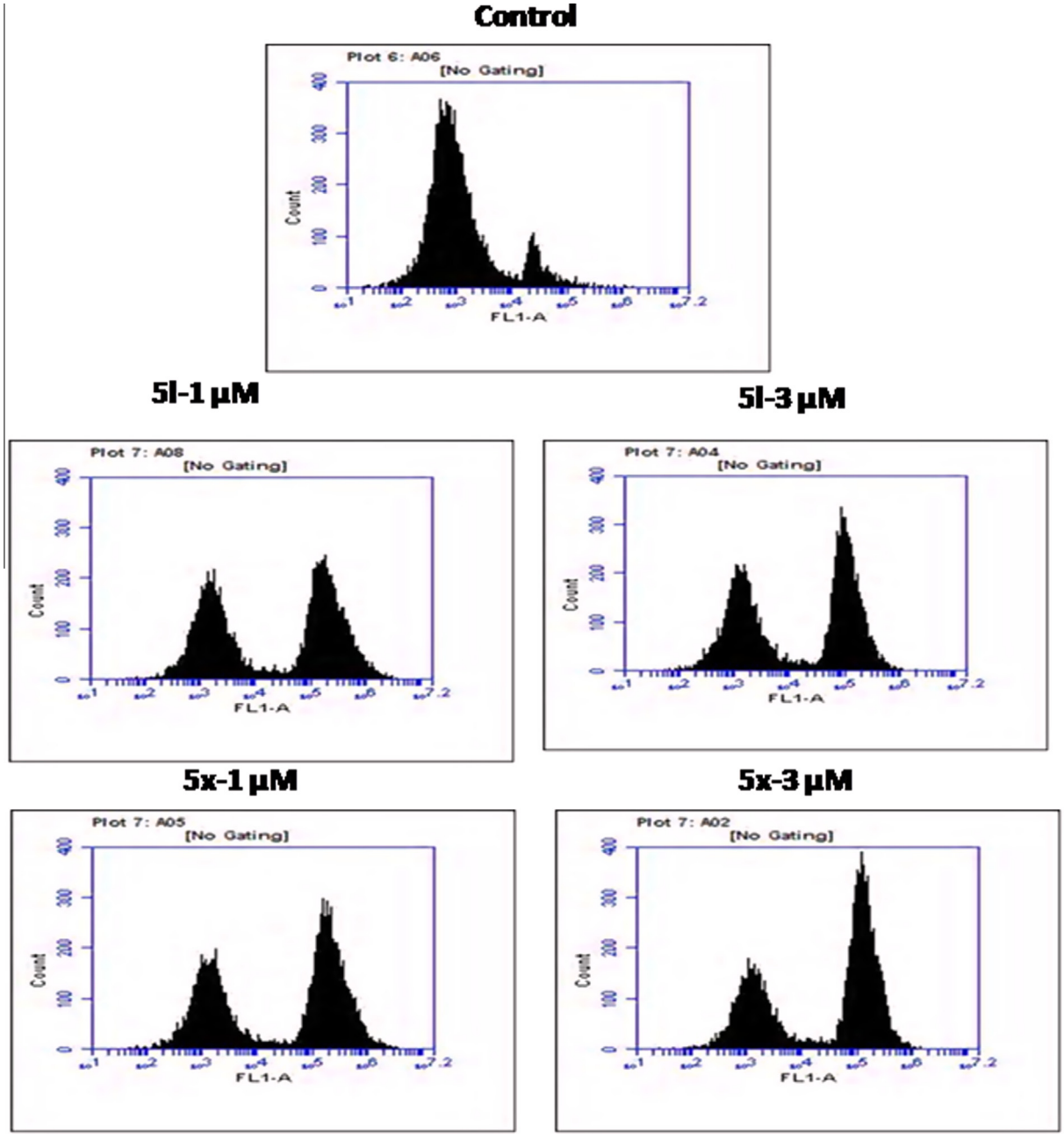

Figure 2A. FACS analysis of cell cycle distribution of MCF-7 cells after treatment with **5l** and **5x** conjugates at 1 µM and 3 µM concentrations for 48 h. Cell cycle analysis was performed by employing propidium iodide as indicated under materials and methods. The percentage of cells in each phase of cell cycle was quantified by flow cytometry.

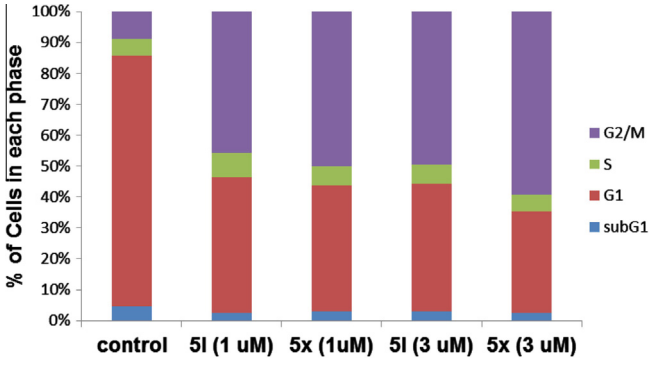

Figure 2B. Distribution of cells at G1, S and G2/M phase of cell cycle analysis with **5l** and **5x** in MCF-7 cell.

Table 4
Antitubulin activity of compounds **5l** and **5x**

Compound	IC_{50}[a] (µM)	% inhibition[b]
5x	1.8	55.6
5l	1.5	52.1
Nocodazole	1.7	58.6

[a] Half maximal inhibitory concentration: compound concentration required to inhibit tubulin polymerization by 50%; data are the mean ± SD of $n = 3$ independent experiments performed in triplicate.

[b] Inhibition of tubulin polymerization at 3 µm (final volume = 10 mL); compounds were pre-incubated with tubulin at a final concentration of 10 µm.

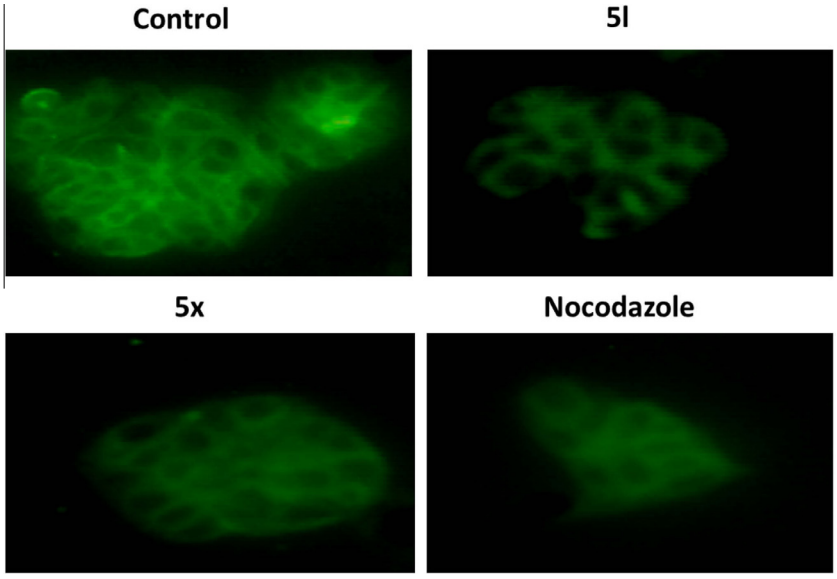

Figure 3. Immunohistochemistry (IHC) analyses of compounds on the microtubule network: MCF-7 cells were treated with compounds **5l**, **5x**, and nocodazole at 1 μM concentration for 48 h followed by staining with α-tubulin antibody. Microtubule organization was clearly observed by green color tubulin network like structures in control cells and was found to be disrupted in cells treated with compounds **5l** and **5x** with nocodazole as positive control.

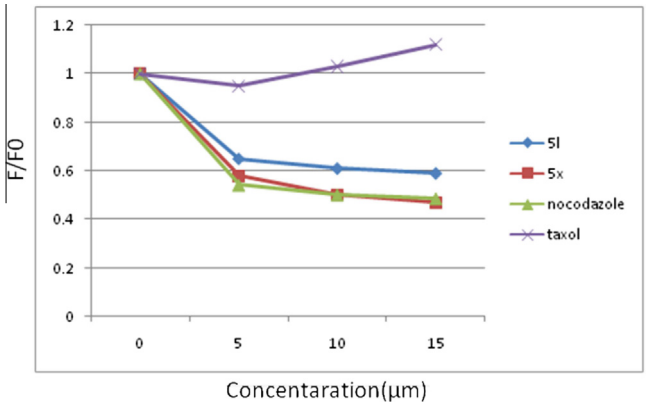

Figure 4. Fluorescence based competitive colchicine binding assay of conjugates **5l** and **5x** were carried out at various concentrations containing 5 μM of tubulin and colchicine for 60 min at 37 °C. Nocodazole was used as a positive control whereas taxol was used as negative control which binds at the taxane site. Fluorescence values are normalized to control.

3.6. Effect on chromatin condensation

It is well-known that the cell cycle arrest at G2/M phase is shown to induce cellular apoptosis.[23] Hence, it was considered of interest to investigate whether the cytotoxicity of these conjugates (**5l** and **5x**) is by virtue of apoptotic cell death. During apoptosis, nuclear fragmentation and chromatin condensation takes place; therefore Hoechst-33242 staining was used to visualize nuclear condensation. It was observed that the 3-(4-(1*H*-benzo[*d*]imidazol-2-yl)phenyl)-5-phenyl-1,2,4-oxadiazole conjugates **5l** and **5x** caused significant nuclear condensation in MCF-7 cells upon treatment at 1 μM concentration for 24 h which is comparable to that of reference standard nocodazole (Fig. 5).

3.7. Effect on mitochondrial membrane potential

Mitochondria plays an essential role in the propagation of apoptosis and its dysfunction within the apoptotic process is often associated with loss or depolarization of mitochondrial membrane potential (DΨm), which leads to collapse of mitochondrial functions ensuing cell death.[24] Therefore, in this study we examined the effect of 3-(4-(1*H*-benzo[*d*]imidazol-2-yl)phenyl)-5-phenyl-1,2,4-oxadiazole conjugates on DΨm. The MCF-7 cells were treated with **5l** and **5x** at 1 μm concentration for 24 h and stained with JC-1 dye. In control cells the dye concentrates in the mitochondrial matrix where it forms red fluorescent aggregates (J-aggregates) because of the electrochemical potential gradient. In cells treated with compounds which induce apoptosis, the mitochondrial membrane is depolarized thus preventing the accumulation of the JC-1 dye in the mitochondria. Therefore, the dye in the monomeric form is dispersed throughout the entire cell leading to a shift from red (J-aggregates) to green fluorescence (JC-1 monomers). Thus, apoptotic cells showing primarily green fluorescence are easily differentiated from healthy cells which show red and green fluorescence. It was observed that these conjugates significantly depolarize the mitochondrial membrane potential (Fig. 6A) as indicated by the green fluorescence in the cells treated by these conjugates, whereas control (untreated cells) showed red colored florescence because of intact mitochondrial membrane potential. Further, the loss of mitochondrial membrane potential was quantified by flow cytometry. As shown in Figure 6B, there is a remarkable shift in the green fluorescence that has increased to 24.0% and 25.7% compared with control cells which is showing 2.2%, indicating that **5l** and **5x** induces apoptosis through depolarization of the mitochondrial membrane potential in MCF-7 cells.

3.8. DNA fragmentation analysis

Endonuclease mediated cleavage of nuclear DNA results in the formation of oligonucleosomal DNA fragment (180–200 base pairs long), a biochemical hallmark of apoptosis.[25] DNA laddering assay was performed on MCF-7 cells treated with 2 μM concentration of the compounds **5l** and **5x**. The chromosomal DNA extracted from MCF-7 cells and used for agarose gel electrophoresis. The results from the Figure 7 indicated that **5l** and **5x** induces DNA fragmentation in MCF-7 treated cells which lead to a smear formation in gel lanes.

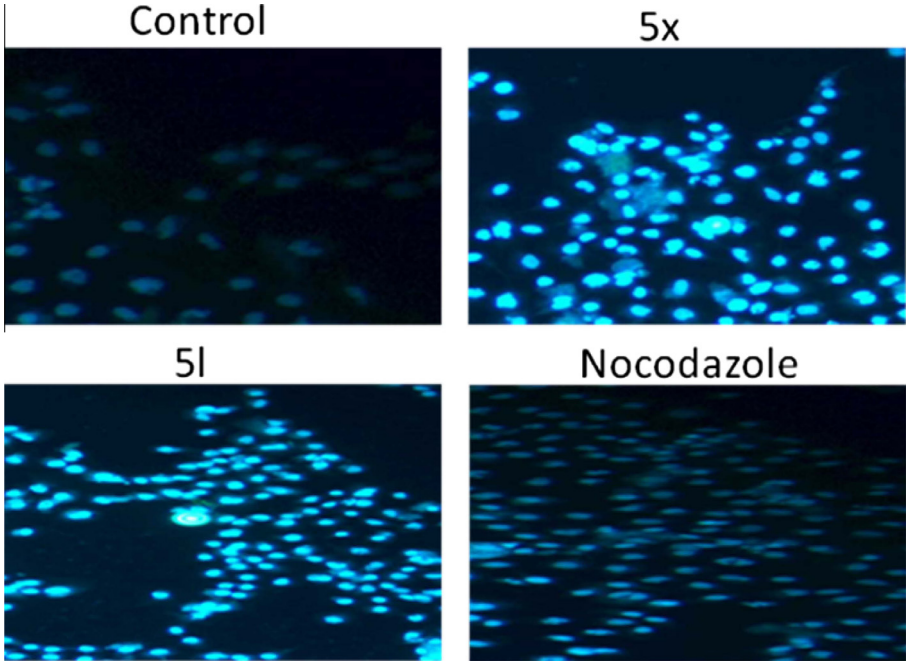

Figure 5. Compounds **5l** and **5x** induced apoptosis in MCF-7 cells. Cells were treated with **5l** and **5x** for 24 h, then washed with PBS and incubated with Hoechst-33258 stain for 20 min to observe nuclear condensation. Fluorescence images were captured with a DAPI filter.

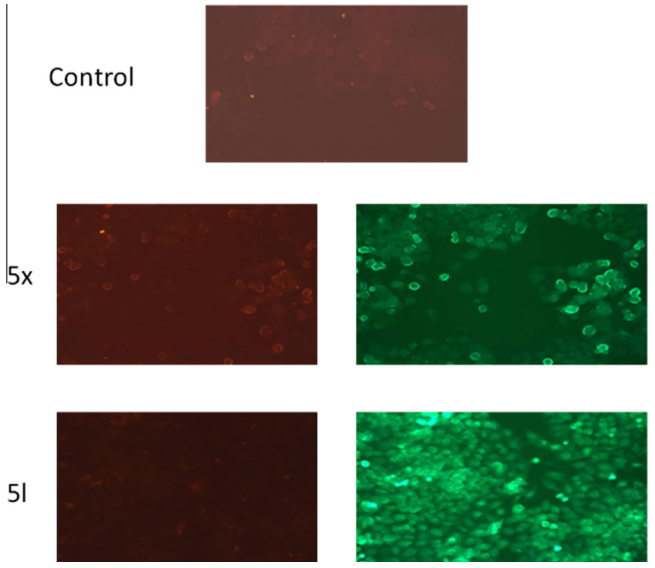

Figure 6A. Compounds **5l** and **5x** cause mitochondrial membrane depolarization in MCF-7 cells. Cells were treated with **5l** and **5x** for 24 h, and mitochondrial membrane potential was measured by JC-1 staining as described in the Section 7.7.

3.9. Annexin V(FITC)-propidium iodide dual staining assay

The apoptotic inducing ability of the conjugates **5l** and **5x** was also investigated by Annexin V FITC/PI (AV/PI) dual staining assay to examine the occurrence of phosphatidylserine externalization and also to understand whether it is due to physiological apoptosis or nonspecific necrosis.[26] In this study, the MCF-7 cells were treated with **5l** and **5x** for 24 h at 1 μM concentration to examine the apoptotic effect. It was observed that these compounds showed significant apoptotic effect against MCF-7 cells. As shown in Figure 8, the compounds **5l** and **5x** showed 16.9% and 17.7% of apoptotic cells, respectively, whereas 2.2% of apoptotic cells were observed in the control (untreated cells). This experiment further suggests that these compounds significantly induced apoptosis in MCF-7 cells.

4. Molecular docking studies

To investigate the possible mode of binding of these new conjugates, we carried out docking studies of conjugates **5l** and **5x** in the colchicines binding site of α,β-tubulin (PDB: 3E22). Conjugates **5l** and **5x** were docked using Auto dock 4.2 docking tool,[27–30] which implements a genetic algorithm based search method. As depicted in Figure 9, the conjugates **5l** and **5x** shared the binding pocket of colchicine displaying interactions with βCys241, βMet259, βIle378, βLys352, βAsn249, αThr179, αSer178 and αGlu71 in the α,β-tubulin.

Docking studies showed that conjugates **5l** and **5x** occupied the colchicine binding site of α,β-tubulin mostly buried in the β-subunits (Fig. 10). The trimethoxy phenyl group of these conjugates occupies the hydrophobic binding site in the tubulin with βLys352, βMet259 and βCys241. Some hydrogen-bonding interactions were observed between their benzimidazole ring with that of βAsn249, βAsn258 and αAsn101 in the range of 2.3–2.9 Å. Furthermore, some electrostatic interactions were also observed in between benzimidazole ring and αAsp98. Whereas oxadiazole ring of these conjugates is involved in the hydrophobic interactions with αThr179 apart from π–π^* stacking interaction with βAsn258. In addition, the 4-methoxy group on benzimidazole ring is involved in hydrogen-binding with that of αGlu71.

5. Conclusion

In conclusion, a series of new 3-(4-(1*H*-benzo[*d*]imidazol-2-yl)phenyl)-5-phenyl-1,2,4-oxadiazole conjugates **5a–x** were synthesized and tested for their antiproliferative activity. Most of the compounds showed moderate to remarkable cytotoxic activity against all the tested tumor cell lines. Two of the conjugates **5l** and **5x** have emerged as potential candidates with broad spectrum of cytotoxic activity against most of the tumor cell lines. The flow

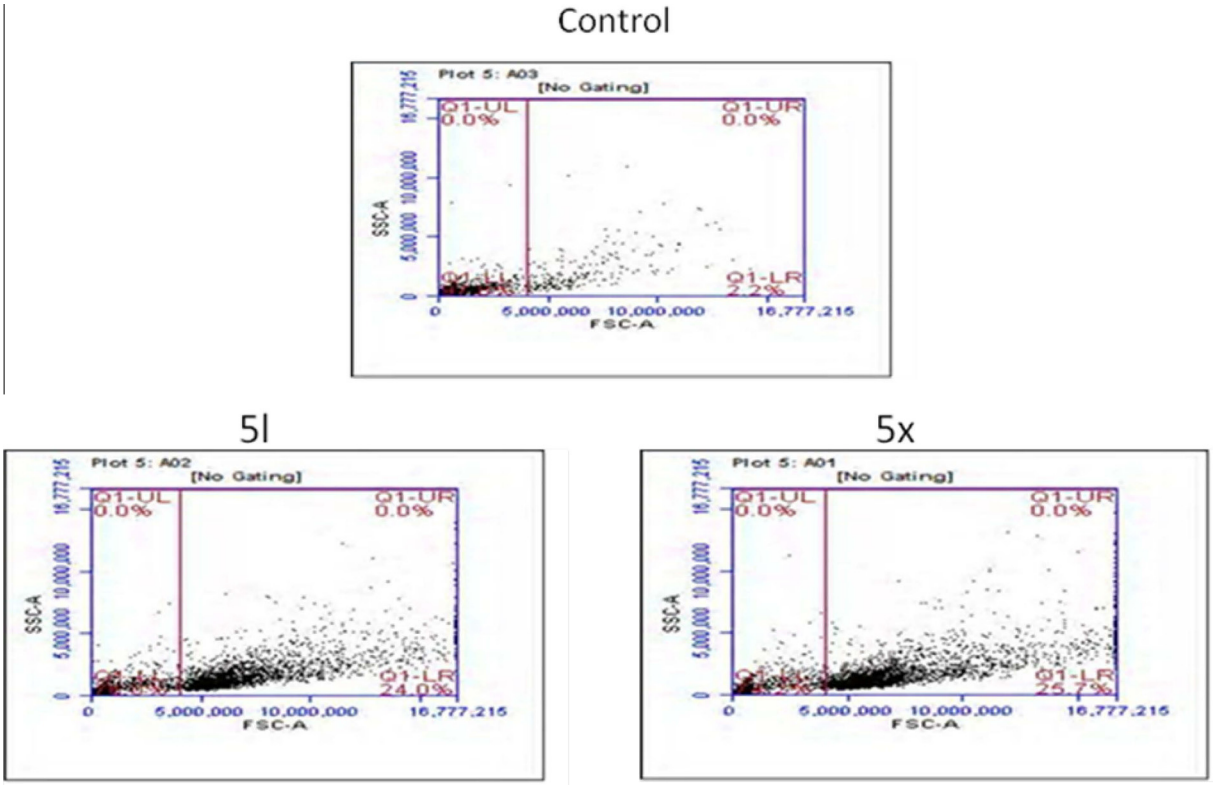

Figure 6B. Assessment of $\Delta\psi_m$ (mitochondrial depolarization) of compounds **5l** and **5x** in MCF-7 cells. Representative histograms of control cells and cells incubated for 24 h in the presence of **5l** and **5x** as indicated, and stained with the fluorescent probe JC-1 after treatment.

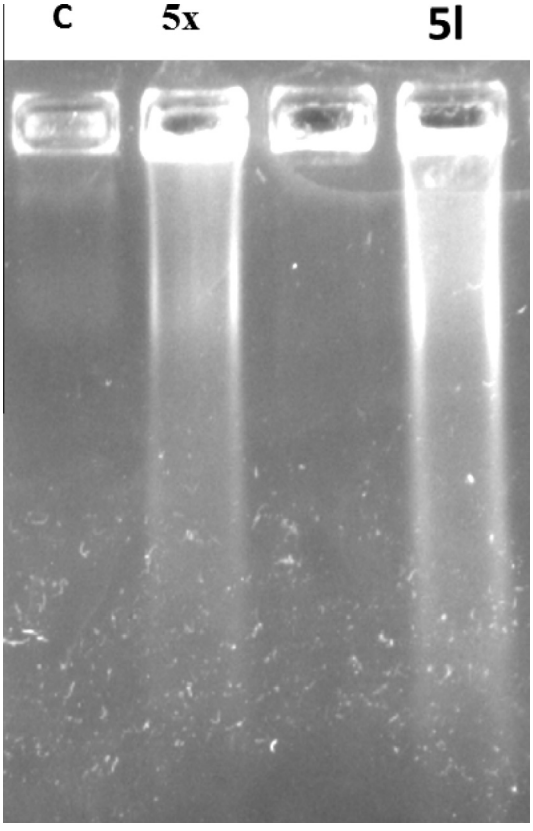

Figure 7. Detection of DNA damage induced by **5x** and **5l** in MCF-7 cells. The chromosomal DNA was extracted from MCF-7 cells treated with 2 μM concentrations of **5x** and **5l** and subjected to agarose gel electrophoresis.

cytometric analysis indicated that they induced G2/M cell cycle arrest in MCF-7 cells and inhibited tubulin polymerization comparable to a reference standard nocodazole apart from disruption of microtubule network formation. Apoptosis induced by these compounds was also determined by characteristic morphological changes such as DNA fragmentation and chromatin condensation. Furthermore, depolarization of mitochondrial membrane potential (MMP) was also observed, which indicated that the mitochondrial pathway was also involved in the apoptosis signaling pathway. The molecular modeling study on tubulin demonstrated that these molecules bind well with the tubulin and are involved in a series of interactions with the proteins. Thus these conjugates could be considered as potential leads in the development of a new class of antimitotic anti-cancer agents.

6. Experimental section

All the reagents, solvents used were of commercial grade and were used without any further purification. The progress of the reactions was monitored by thin layer chromatography (TLC), performed on silica gel glass plates containing 60 F-254, and visualization on TLC was achieved by UV light or iodine indicator. Melting points were measured with an Electrothermal melting point apparatus, and are uncorrected. ^{1}H and ^{13}C NMR spectra were recorded on INOVA (400 MHz) or Gemini Varian-VXR-unity (200 MHz) or Bruker UXNMR/XWIN-NMR (300 MHz) instruments. Chemical shifts (δ) are reported in ppm downfield from internal TMS standard. Signal multiplicities are represented by s (singlet), d (doublet), t (triplet), ds (double singlet), dd (double doublet), m (multiplet) and br s (broad singlet). ESI spectra were recorded on Micro mass, Quattro LC using ESI+ software with capillary voltage 3.98 kV and ESI mode positive ion trap detector. IR spectra were recorded on KBr disk using a FTIR bruker Vector 22 Spectrophotometer.

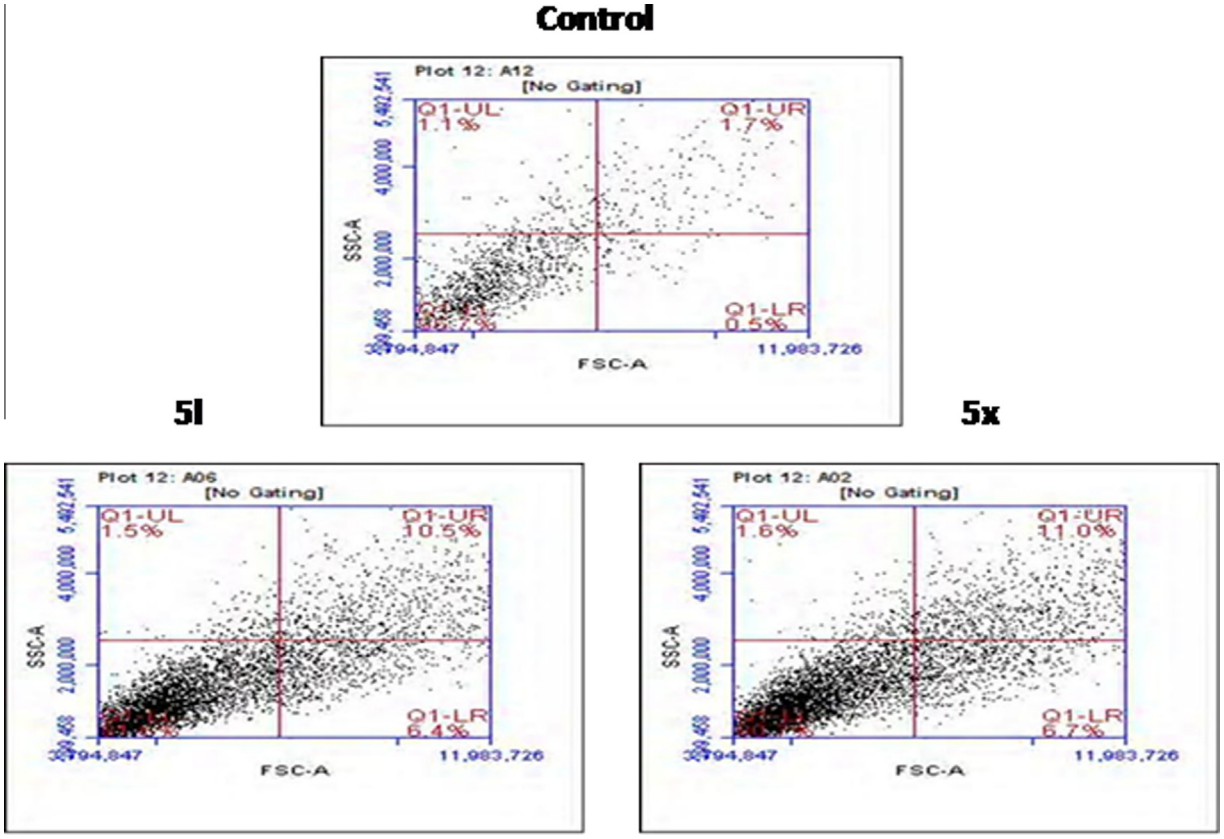

Figure 8. Representative histograms of MCF-7 cells treated with compounds **5l** and **5x** for 24 h and analyzed by flow cytometry after double staining of the cells with Annexin-V-FITC and PI.

6.1. General procedure for the synthesis of 4-(1*H*-benzo[*d*]imidazol-2-yl)benzonitrile 8 (a–d)

The starting nitrile compounds **8** (**a**–**d**) were prepared according to the literature method. To a mixture of appropriate *o*-phenylenediamines **7a**–**d** (0.5 mmol) and 4-cyano benzaldehyde **6** (0.5 mmol) in ethanol was added a solution of $Na_2S_2O_5$ (4 mmol) in H_2O (1.6 mL). The resulting mixture was stirred at reflux for 4 h, after completion of reaction; the solution was poured onto crushed ice. The resulting solid was filtered, washed with cold water, dried and recrystallized from ethanol to afford compounds **8**(**a**–**d**). Among the synthesized 4-(1*H*-benzo[*d*]imidazol-2-yl)benzonitriles **8**(**a**–**d**), compounds **8b** and **8d** were reported for the first time and were characterized by NMR (^{1}H, ^{13}C) and the physical and spectral data of the compounds **8a** and **8c** were in complete agreement with the reported data.[31]

6.1.1. 4-(5-Fluoro-1*H*-benzo[*d*]imidazol-2-yl)benzonitrile (8b)

This compound was prepared by method described in Section 6.1 employing 4-cyano benzaldehyde (1.31 g, 1 mmol) and 4-flouro-*o*-phenylenediamine (1.26 mg, 1 mmol) to afford **8b**, as light yellow solid 1.65 g, in 69% yield. Mp 218–221 °C. ^{1}H NMR (300 MHz, DMSO) δ 7.12 (d, 1H, J = 7.65 Hz), 7.52 (s, 1H), 7.67 (d, 1H, J = 7.71 Hz), 8.02 (d, 2H, J = 8.3 Hz), 8.13 (d, 2H, J = 8.3 Hz). MS (ESI): m/z 238 $[M+H]^+$.

6.1.2. 4-(5-Methoxy-1*H*-benzo[*d*]imidazol-2-yl)benzonitrile (8d)

This compound was prepared by method described in Section 6.1 employing 4-cyano benzaldehyde (1.31 g, 1 mmol) and 4-methoxy-*o*-phenylenediamine (1.38 g, 1 mmol) to afford **8d**, as light yellow solid, 1.66 g, in 66% yield. Mp 205–207 °C. ^{1}H NMR (300 MHz, DMSO) δ 3.81 (s, 3H), 6.92 (d, 1H, J = 7.29 Hz), 7.21 (s, 1H), 7.58 (d, 1H, J = 7.27 Hz), 8.08 (d, 2H, J = 8.24 Hz), 8.21 (d, 2H, J = 8.26 Hz). MS (ESI): m/z 250 $[M+H]^+$.

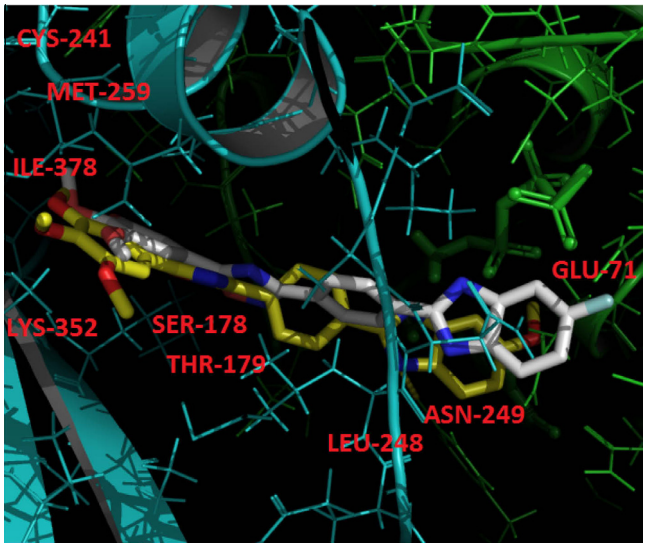

Figure 9. Superposition of the conjugate **5x** (yellow stick) and **5l** (gray stick) in the colchicine binding site of tubulin (with βCys241, βMet259, βIle378, βLys352, βLeu248, βAsn249, αThr179 and αGlu71) with β-chain in cyan color, α-chain in green color, N-atom (blue color) and O-atom (red color).

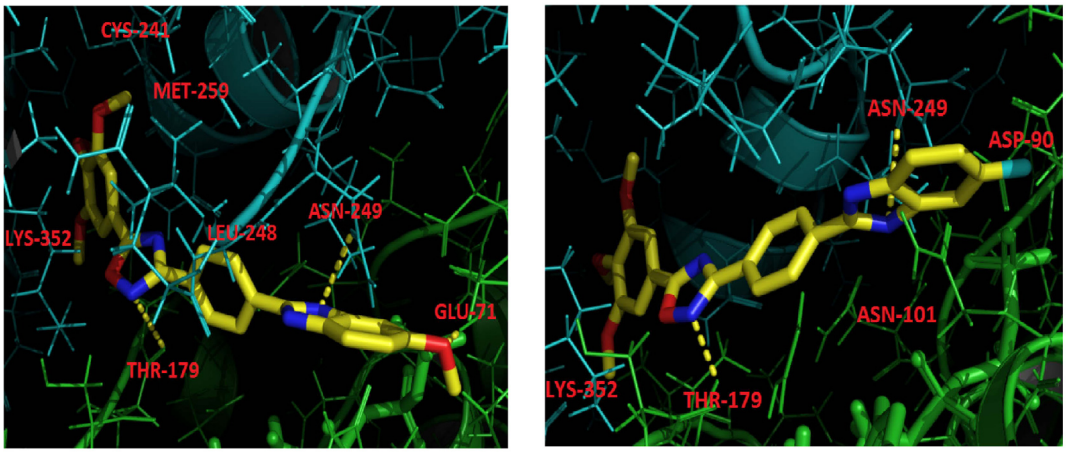

5x **5l**

Figure 10. Binding pose of the conjugate **5x** (yellow stick) and **5l** (yellow stick) in the colchicine binding site of tubulin (with βCys241, βLys352, αThr179 and βAsn101) with β-chain in cyan color, α-chain in green color, N-atom (blue color) and O-atom (red color).

6.2. General procedure for the synthesis of (*Z*)-4-(1*H*-benzo[*d*]imidazol-2-yl)-*N*′-hydroxybenzimidamide 9(a–d)

To a solution of appropriate benzonitrile (1.0 mmol) in ethanol (5 mL) was added hydroxylamine hydrochloride (1.1 mmol, 764 mg) and sodium hydroxide (1.1 mmol, 444 mg), each dissolved in water (10 mL) sequentially, for a period of 20 min at 0 °C. Then the resulting mixture was allowed to reflux with stirring for 18 h. The pH of the solution was adjusted to 2 with 1 N HCl and the aqueous phase was washed with ethyl acetate (2 × 35 mL). Upon cooling (0 °C) and neutralization with sodium bicarbonate gave precipitate which was filtered, washed and dried to afford pure amidoximes **9**(**a**–**d**).

6.2.1. (*Z*)-4-(1*H*-Benzo[*d*]imidazol-2-yl)-*N*′-hydroxybenzimidamide (9a)

This compound was prepared by method described in Section 6.2 employing 4-(1*H*-benzo[*d*]imidazol-2-yl)benzonitrile (**8a**, 2.18 g, 1 mmol) to afford **9a** as light brown solid, 1.87 g, in 74% yield. Mp 227–229 °C. ^{1}H NMR (300 MHz, DMSO) δ 5.57 (s, 2H), 7.11–7.29 (m, 2H), 7.65–7.74 (m, 2H), 7.89 (d, 2H, J = 8.12 Hz), 8.24 (dd, 4H, J = 8.32, 5.65 Hz), 9.31 (s, 1H). ^{13}C NMR (75 MHz, DMSO) δ 162.3, 154.1, 151.8, 139.7, 139.5, 135.6, 128.4, 127.2, 123.6, 123.4, 116.3, 114.9. MS (ESI): m/z 253 $[M+H]^+$.

6.2.2. 9(*Z*)-4-(5-Fluoro-1*H*-benzo[*d*]imidazol-2-yl)-*N*′-hydroxybenzimidamide (9b)

This compound was prepared by method described in Section 6.2 employing 4-(5-fluoro-1*H*-benzo[*d*]imidazol-2-yl)benzonitrile (**8b**, 2.37 g, 1 mmol) to afford **9b** as off light brown solid 2.06 g, in 76% yield. Mp 223–225 °C. ^{1}H NMR (300 MHz, DMSO) δ 5.61 (br s, 2H), 7.11 (d, 1H, J = 7.63 Hz), 7.47 (s, 1H), 7.66 (d, 1H, J = 7.67 Hz), 7.97 (d, 2H, J = 8.27 Hz), 8.14 (d, 2H, J = 8.26 Hz), 9.35 (s, 1H). ^{13}C NMR (75 MHz, DMSO) δ 162.5, 155.7, 154.0, 151.9, 138.7, 135.7, 134.2, 128.6, 127.3, 116.1, 11.4, 103.3. MS (ESI): m/z 271 $[M+H]^+$.

6.2.3. (*Z*)-4-(5-Chloro-1*H*-benzo[*d*]imidazol-2-yl)-*N*′-hydroxybenzimidamide (9c)

This compound was prepared by method described in Section 6.2 employing 4-(5-chloro-1*H*-benzo[*d*]imidazol-2-yl)benzonitrile (**8c**, 2.49 g, 1 mmol) to afford **9c** as brown solid 2.21 g, in 77% yield. Mp 236–238 °C. ^{1}H NMR (300 MHz, DMSO) δ 5.58 (br s, 1H), 7.14 (d, 1H, J = 8.49 Hz), 7.41–7.60 (m, 2H), 7.92 (d, 2H, J = 8.30 Hz), 8.16 (d, 2H, J = 8.49 Hz) 9.30 (s, 1H). ^{13}C NMR (75 MHz, DMSO) δ 162.3, 154.2, 151.7, 137.7, 135.9, 133.5, 129.8, 128.6, 127.4, 123.3, 116.7, 116.3. MS (ESI): m/z 287 $[M+H]^+$.

6.2.4. (*Z*)-*N*′-Hydroxy-4-(5-methoxy-1*H*-benzo[*d*]imidazol-2-yl)benzimidamide (9d)

This compound was prepared by method described in Section 6.2 employing (4-(5-methoxy-1*H*-benzo[*d*]imidazol-2-yl)benzonitrile) (**8d**, 2.49 g, 1 mmol) to afford **9d** as light yellow solid 1.97 g, in 69% yield. Mp 218–221 °C. ^{1}H NMR (300 MHz, DMSO) δ 3.78 (s, 3H), 5.51 (s, 2H), 6.92–7.18 (m, 2H), 7.61 (d, 1H, J = 7.26 Hz), 8.02 (d, 2H, J = 8.26 Hz), 8.17 (d, 2H, J = 8.26 Hz), 9.35 (s, 1H).^{13}C NMR (75 MHz, DMSO) δ 162.3, 155.8, 154.3, 151.8, 138.6, 136.1, 135.5, 128.6, 127.7, 114.6, 113.2, 101.7. MS (ESI): m/z 283 $[M+H]^+$.

6.3. General procedure for the synthesis of compounds 5(a–x)

To a solution of appropriate carboxylic acid (0.5 mmol) in dry DMF (3 mL) was added Carbonyl diimidazole (0.6 mmol) under nitrogen atmosphere and the reaction mixture was stirred at room temperature for 1 h. Then appropriate amidoxime **9a**–**d** (0.6 mmol) was added and reaction mixture was heated at 110 °C for about 18 h (monitored by TLC). The contents of the reaction were cooled to 25 °C and poured into ice-cold water (25 mL), extracted by ethyl acetate (3 × 15.0 mL) and the combined organic phase was washed with brine, dried over anhydrous sodium sulfate, filtered and concentrated in vacuo. The obtained residue was purified by column chromatography using ethyl acetate–hexane (0–30%) as eluent to furnish pure 1,2,4-oxadiazoles **5**(**a**–**x**) in moderate yields.

6.3.1. (3-(4-(1*H*-Benzo[*d*]imidazol-2-yl)phenyl)-5-phenyl-1,2,4-oxadiazole) 5a

This compound was prepared by method described in Section 6.3 employing ((*Z*)-4-(1*H*-benzo[*d*]imidazol-2-yl)-*N*′-hydroxybenzimidamide) **9a** (152 mg, 0.6 mmol) and benzoic acid (61 mg, 0.5 mmol) to afford **5a** as off white solid 121 mg, in 59% yield. Mp 187–189 °C. ^{1}H NMR (300 MHz, $CDCl_3$) δ 5.38 (br s, 1H), 7.01 (dd, 2H, J = 6.0, 3.1 Hz), 7.29–7.49 (m, 4H), 7.63–7.67 (m, 1H), 8.00 (d, 2H, J = 7.9 Hz), 8.06 (d, 2H, J = 8.2 Hz), 8.14 (d, 2H, J = 8.5 Hz); ^{13}C NMR (125 MHz, $CDCl_3$) δ 174.8, 167.9, 151.3, 138.7, 138.5, 134.6, 130.2, 128.9, 128.4, 128.2, 127.2, 126.8, 126.6, 123.5, 123.3, 116.4, 116.2. MS (ESI): m/z 339 $[M+H]^+$. HRMS (ESI) calcd for $C_{21}H_{14}N_4O$ $[M+H]^+$ 339.12471; found: 339.12132.

6.3.2. (3-(4-(1*H*-Benzo[*d*]imidazol-2-yl)phenyl)-5-(4-fluorophenyl)-1,2,4-oxadiazole) 5b

This compound was prepared by method described in Section 6.3 employing ((*Z*)-4-(1*H*-benzo[*d*]imidazol-2-yl)-*N*′-hydroxybenzimidamide) **9a** (152 mg, 0.6 mmol), 4-flouro benzoic acid (70 mg, 0.5 mmol) to afford **5b** as off white solid 115 mg, in 53% yield. Mp 181–183 °C. ^{1}H NMR (300 MHz, $CDCl_3$) δ 5.29 (br s, 1H), 7.16–7.24 (m, 2H), 7.50–7.55 (m, 2H), 7.56 (d, 2H, J = 8.23 Hz), 7.92 (d, 2H, J = 8.23 Hz), 8.19–8.30 (m, 4H); ^{13}C NMR (125 MHz, $CDCl_3$) δ 174.9, 167.9, 164.9, 151.3, 138.8, 138.5, 134.7, 130.2, 128.5, 128.3, 127.1, 124.0, 123.6, 123.3, 116.4, 116.1, 115.8. MS (ESI): m/z 357 $[M+H]^+$. HRMS (ESI) calcd for $C_{21}H_{14}FN_4O$ $[M+H]^+$ 357.11508; found: 357.11463.

6.3.3. (3-(4-(1*H*-Benzo[*d*]imidazol-2-yl)phenyl)-5-(4-chlorophenyl)-1,2,4-oxadiazole) 5c

This compound was prepared by method described in Section 6.3 employing ((*Z*)-4-(1*H*-benzo[*d*]imidazol-2-yl)-*N*′-hydroxybenzimidamide) **9a** (152 mg, 0.6 mmol), *p*-chloro benzoic acid (78 mg, 0.5 mmol) to afford **5c** as off white solid 127 mg, in 56% yield. Mp 195–196 °C. ^{1}H NMR (500 MHz, $CDCl_3$) δ 5.32 (br s, 1H), 7.18–7.24 (m, 2H), 7.52–7. 63 (m, 4H), 7.87 (d, 2H, J = 8.12 Hz), 8.18–8.30 (dd, 4H, J = 8.30, 5.61 Hz); ^{13}C NMR (125 MHz, $CDCl_3$) δ 174.8, 168.0, 151.2, 138.8, 138.4, 138.1, 134.6, 129.7, 129.4, 128.5, 128.4, 127.3, 127.1, 123.5, 123.3, 116.3, 116.1. MS (ESI): m/z 373 $[M+H]^+$. HRMS (ESI) calcd for $C_{21}H_{14}ClN_4O$ [M+H]+ 373.08481; found: 373.08495.

6.3.4. (3-(4-(1*H*-Benzo[*d*]imidazol-2-yl)phenyl)-5-(4-methoxyphenyl)-1,2,4-oxadiazole) 5d

This compound was prepared by method described in Section 6.3 employing ((*Z*)-4-(1*H*-benzo[*d*]imidazol-2-yl)-*N*′-hydroxybenzimidamide) **9a** (152 mg, 0.6 mmol), *p*-methoxy benzoic acid (76 mg, 0.5 mmol) to afford **5d** as light yellow solid 108 mg, in 48.6% yield. Mp 197–201 °C. ^{1}H NMR (300 MHz, $CDCl_3$) δ 3.84 (s, 3H), 5.29 (br s, 1H), 6.89 (d, 2H, J = 8.68 Hz), 7.21–7.42 (m, 4H), 7.81 (d, 2H, J = 8.12 Hz), 8.19–8.28 (m, 4H); ^{13}C NMR (125 MHz, $CDCl_3$) δ 174.8, 167.9, 161.3, 151.1, 138.6, 138.2, 134.6, 128.6, 128.4, 127.0, 125.6, 123.4, 123.2, 118.9, 116.3, 116.1, 114.2, 56.0. MS (ESI): m/z 369 $[M+H]^+$. HRMS (ESI) calcd for $C_{22}H_{17}N_4O_2$ [M+H]+ 369.13495; found: 369.13482.

6.3.5. (3-(4-(1*H*-Benzo[*d*]imidazol-2-yl)phenyl)-5-*p*-tolyl-1,2,4-oxadiazole) 5e

This compound was prepared by method described in Section 6.3 employing ((*Z*)-4-(1*H*-benzo[*d*]imidazol-2-yl)-*N*′-hydroxybenzimidamide) **9a** (152 mg, 0.6 mmol), *p*-tolylbenzoic acid (68 mg, 0.5 mmol) to afford **5e** as off white solid 103 mg, in 48.3% yield. Mp 182–184 °C. ^{1}H NMR (500 MHz, $CDCl_3$) δ 2.39 (s, 3H), 5.21 (br s, 1H), 7.21–7.36 (m, 4H), 7.51 (d, 2H, J = 8.87 Hz), 7.58–7.64 (m, 2H), 8.20–8.29 (m, 4H); ^{13}C NMR (125 MHz, $CDCl_3$) δ 174.7, 167.8, 151.1, 141.1, 138.6, 138.4, 134.4, 129.1, 128.4, 128.2, 127.7, 127.1, 125.7, 123.5, 123.3, 116.3, 116.2, 21.2. MS (ESI): m/z 353 $[M+H]^+$; HRMS (ESI) calcd for $C_{22}H_{17}N_4O$ $[M+H]^+$ 353.14002; found: 353.14034.

6.3.6. (3-(4-(1*H*-Benzo[*d*]imidazol-2-yl)phenyl)-5-(3,4,5-trimethoxyphenyl)-1,2,4-oxadiazole) 5f

This compound was prepared by method described in Section 6.3 employing ((*Z*)-4-(1*H*-benzo[*d*]imidazol-2-yl)-*N*′-hydroxybenzimidamide) **9a** (152 mg, 0.6 mmol), 3,4,5-methoxy benzoic acid (106 mg, 0.5 mmol) to afford **5f** as light yellow solid 146 mg, in 56.5% yield. Mp 187–189 °C. ^{1}H NMR (300 MHz, $CDCl_3$) δ 3.87 (s, 3H), 3.91 (s, 6H), 5.27 (br s, 1H), 7.04 (s, 2H), 7.20–7.31 (m, 2H), 7.41–7.49 (m, 2H), 8.19–8.28 (dd, 4H, J = 8.30, 7.93 Hz); ^{13}C NMR (125 MHz, $CDCl_3$) δ 174.8, 167.9, 151.4, 151.2, 143.2, 138.6, 138.5, 134.4, 129.1, 128.4, 127.0, 123.4, 123.3, 121.9, 116.3, 116.2, 106.8, 60.7, 56.3. MS (ESI): m/z 429 $[M+H]^+$. HRMS (ESI) calcd for $C_{24}H_{21}N_4O_4$ $[M+H]^+$ 429.15627; found: 429.15616.

6.3.7. (3-(4-(5-Fluoro-1*H*-benzo[*d*]imidazol-2-yl)phenyl)-5-phenyl-1,2,4-oxadiazole) 5g

This compound was prepared by method described in Section 6.3 employing 9(*Z*)-4-(5-fluoro-1*H*-benzo[*d*]imidazol-2-yl)-*N*′-hydroxybenzimidamide) **9b** (162 mg, 0.6 mmol), benzoic acid (61 mg, 0.5 mmol) to afford **5g** as light brown solid 127 mg, in 59.6% yield. Mp 177–179 °C. ^{1}H NMR (300 MHz, $CDCl_3$) δ 5.31 (br s, 1H), 7.02 (d, 1H, J = 7.29 Hz), 7.32–7.41 (m, 4H), 7.59 (d, 1H, J = 7.29 Hz), 7.79 (d, 2H, J = 8.12 Hz), 8.19–8.30 (m, 4H); ^{13}C NMR (125 MHz, $CDCl_3$) δ 174.8, 167.9, 155.9, 151.2, 139.6, 134.6, 133.2, 130.2, 128.8, 128.4, 128.1, 127.2, 126.7, 126.5, 116.2, 112.8, 103.9. MS (ESI): m/z 357 $[M+H]^+$. HRMS (ESI) calcd for $C_{21}H_{14}FN_4O$ $[M+H]^+$ 357.11509; found: 357.11535.

6.3.8. (3-(4-(5-Fluoro-1*H*-benzo[*d*]imidazol-2-yl)phenyl)-5-(4-fluorophenyl)-1,2,4-oxadiazole) 5h

This compound was prepared by method described in Section 6.3 employing 9(*Z*)-4-(5-fluoro-1*H*-benzo[*d*]imidazol-2-yl)-*N*′-hydroxybenzimidamide) **9b** (162 mg, 0.6 mmol), *p*-fluoro benzoic acid (70 mg, 0.5 mmol) to afford **5h** as light brown solid 131 mg, in 58.6% yield. Mp 165–168 °C. ^{1}H NMR (300 MHz, $CDCl_3$) δ 5.31 (br s, 1H), 7.11 (d, 1H, J = 7.26 Hz), 7.36–7.45 (m, 3H) 7.61 (s, 1H), 7.83 (d, 2H, J = 8.28 Hz), 8.21–8.33 (m, 4H); ^{13}C NMR (125 MHz, $CDCl_3$) δ 174.9, 167.9, 164.9, 155.9, 151.2, 139.6, 134.6, 133.1, 130.1, 128.4, 128.2, 127.1, 123.9, 116.2, 115.8, 112.9, 103.8. MS (ESI): m/z 375 $[M+H]^+$. HRMS (ESI) calcd for $C_{21}H_{13}F_2N_4O$ [M+H]+ 375.10556; found: 375.10545.

6.3.9. (5-(4-Chlorophenyl)-3-(4-(5-fluoro-1*H*-benzo[*d*]imidazol-2-yl)phenyl)-1,2,4-oxadiazole) 5i

This compound was prepared by method described in Section 6.3 employing 9(*Z*)-4-(5-fluoro-1*H*-benzo[*d*]imidazol-2-yl)-*N*′-hydroxybenzimidamide) **9b** (162 mg, 0.6 mmol), *p*-chloro benzoic acid (78 mg, 0.5 mmol) to afford **5i** as light brown solid 142 mg, in 60.8% yield. Mp 186–188 °C. ^{1}H NMR (300 MHz, $CDCl_3$) δ 5.31 (br s, 1H), 7.07 (d, 1H, J = 7.3 Hz), 7.41–7.57 (m, 5H) 7.59 (d, 1H, J = 7.3 Hz), 8.21–8.33 (m, 4H); ^{13}C NMR (125 MHz, $CDCl_3$) δ 174.7, 167.9, 155.8, 151.2, 139.7, 138.2, 134.7, 129.7, 129.4, 128.8, 128.4, 127.3, 127.0, 116.1, 133.2, 112.7, 103.9. MS (ESI): m/z 391 $[M+H]^+$. HRMS (ESI) calcd for $C_{21}H^{13}ClFN_4O$ $[M+H]^+$ 391.07613; found: 391.07594.

6.3.10. (3-(4-(5-Fluoro-1*H*-benzo[*d*]imidazol-2-yl)phenyl)-5-(4-methoxyphenyl)-1,2,4-oxadiazole) 5j

This compound was prepared by method described in Section 6.3 employing 9(*Z*)-4-(5-fluoro-1*H*-benzo[*d*]imidazol-2-yl)-*N*′-hydroxybenzimidamide) **9b** (162 mg, 0.6 mmol), *p*-methoxy benzoic acid (76 mg, 0.5 mmol) to afford **5j** as light yellow solid 147 mg, in 63.7% yield. Mp 175–177 °C. ^{1}H NMR (500 MHz, $CDCl_3$) δ 3.89 (s, 3H), 7.08–7.21 (m, 3H), 7.58 (d, 1H, J = 7.24 Hz), 7.68 (s, 1H), 7.91 (d, 2H, J = 8.28 Hz), 8.27–8.32 (m, 4H); ^{13}C NMR (125 MHz, $CDCl_3$) δ 174.9, 167.8, 161.2, 155.7, 151.2, 139.7, 134.6, 133.2, 128.6, 128.4, 126.9, 125.5, 118.8, 116.2, 114.3, 112.8, 103.7, 56.1. MS (ESI): m/z 387 $[M+H]^+$. HRMS (ESI) calcd for $C_{22}H_{16}FN_4O_2$ [M+H]+ 387.12567; found: 387.12551.

6.3.11. (3-(4-(5-Fluoro-1*H*-benzo[*d*]imidazol-2-yl)phenyl)-5-*p*-tolyl-1,2,4-oxadiazole) 5k

This compound was prepared by method described in Section 6.3 employing 9(*Z*)-4-(5-fluoro-1*H*-benzo[*d*]imidazol-2-yl)-*N*′-hydroxybenzimidamide) **9b** (162 mg, 0.6 mmol), *p*-tolyl

benzoic acid (68 mg, 0.5 mmol) to afford **5k** as off white solid 123 mg, in 55.6% yield. Mp 172–175 °C. ^{1}H NMR (300 MHz, $CDCl_3$) δ 2.37 (s, 3H), 7.02–7.25 (m, 3H), 7.57 (d, 1H, J = 7.18 Hz), 7.64 (s, 1H), 7.87 (d, 2H, J = 8.23 Hz), 8.16–8.29 (m, 4H). ^{13}C NMR (125 MHz, $CDCl_3$) δ 175.0, 167.8, 155.6, 151.2, 141.4, 139.7, 134.6, 133.3, 129.3, 128.6, 128.2, 127.7, 127.2, 125.8, 116.4, 112.9, 103.6, 21.3. MS (ESI): m/z 371 $[M+H]^+$. HRMS (ESI) calcd for $C_{22}H_{16}N_4F$ $[M+H]^+$ 371.13067; found: 371.13025.

6.3.12. (3-(4-(5-Fluoro-1*H*-benzo[*d*]imidazol-2-yl)phenyl)-5-(3,4,5-trimethoxyphenyl)-1,2,4-oxadiazole) 5l

This compound was prepared by method described in Section 6.3 employing 9(*Z*)-4-(5-fluoro-1*H*-benzo[*d*]imidazol-2-yl)-*N*′-hydroxybenzimidamide) **9b** (162 mg, 0.6 mmol), 3,4,5-methoxy benzoic acid (106 mg, 0.5 mmol) to afford **5l** as light yellow solid 160 mg, in 60% yield. Mp 166–168 °C. ^{1}H NMR (500 MHz, $CDCl_3$) δ 3.81 (s, 3H), 3.87 (s, 6H), 6.98–7.21 (m, 3H), 7.46 (s, 1H), 7.55 (d, 1H, J = 7.28 Hz), 8.19–8.30 (dd, 4H, J = 8.30, 7.93 Hz); ^{13}C NMR (125 MHz, $CDCl_3$) δ 174.9, 167.8, 155.7, 151.4, 151.1, 143.3, 139.6, 134.3, 133.1, 129.2, 128.3, 127.1, 122.0, 116.4, 112.8, 106.9, 103.8, 60.8, 56.3. MS (ESI): m/z 447 $[M+H]^+$. HRMS (ESI) calcd for $C_{24}H_{20}FN_4O_4$ $[M+H]^+$ 447.14677; found: 447.14642.

6.3.13. 3-(4-(5-Chloro-1*H*-benzo[*d*]imidazol-2-yl)phenyl)-5-phenyl-1,2,4-oxadiazole 5m

This compound was prepared by method described in Section 6.3 employing ((*Z*)-4-(5-chloro-1*H*-benzo[*d*]imidazol-2-yl)-*N*′-hydroxybenzimidamide) **9c** (172 mg, 0.6 mmol), benzoic acid (61 mg, 0.5 mmol) to afford **5m** as off white solid 134 mg, in 60.1% yield. Mp 163–165 °C. ^{1}H NMR (500 MHz, $CDCl_3$) δ 5.28 (br s, 1H), 7.10 (t, 1H, J = 7.27 Hz), 7.13–7.24 (m, 3H), 7.76 (d, 2H, J = 8.27 Hz), 7.96 (d, 2H, J = 8.28 Hz), 8.24 (dd, 4H, J = 8.32, 5.65 Hz). ^{13}C NMR (125 MHz, $CDCl_3$) δ 174.9, 167.8, 151.1, 138.1, 134.7, 133.2, 130.2, 129.7, 128.9, 128.3, 128.2, 127.1, 126.6, 122.9, 116.7, 116.2. MS (ESI): m/z 373 $[M+H]^+$. HRMS (ESI) calcd for $C_{21}H_{14}ClN_4O$ [M+H]+ 373.08556; found: 373.08561.

6.3.14. (3-(4-(5-Chloro-1*H*-benzo[*d*]imidazol-2-yl)phenyl)-5-(4-fluorophenyl)-1,2,4-oxadiazole) 5n

This compound was prepared by method described in Section 6.3 employing ((*Z*)-4-(5-chloro-1*H*-benzo[*d*]imidazol-2-yl)-*N*′-hydroxybenzimidamide) **9c** (172 mg, 0.6 mmol), *p*-fluoro benzoic acid (70 mg, 0.5 mmol) to afford **5n** as light brown solid 127 mg, in 54.4% yield. Mp 156–158 °C. ^{1}H NMR (300 MHz, $CDCl_3$) δ 7.21–7.35 (m, 3H), 7.57 (d, 1H, J = 7.23 Hz), 7.75 (s, 1H), 7.87 (d, 2H, J = 8.30 Hz), 8.26–8.30 (m, 4H); ^{13}C NMR (125 MHz, $CDCl_3$) δ 174.8, 167.9, 164.8, 151.3, 138.2, 134.7, 133.1, 130.1, 129.8, 128.4, 128.2, 127.2, 124.0, 123.0, 116.7, 116.2, 115.8. MS (ESI): m/z 355 $[M+H]^+$. HRMS (ESI) calcd for $C_{21}H^{13}ClFN_4O$ $[M+H]^+$ 391.07578; found: 391.07556.

6.3.15. (3-(4-(5-Chloro-1*H*-benzo[*d*]imidazol-2-yl)phenyl)-5-(4-chlorophenyl)-1,2,4-oxadiazole) 5o

This compound was prepared by method described in Section 6.3 employing ((*Z*)-4-(5-chloro-1*H*-benzo[*d*]imidazol-2-yl)-*N*′-hydroxybenzimidamide) **9c** (172 mg, 0.6 mmol), *p*-chloro benzoic acid (78 mg, 0.5 mmol) to afford **5o** as light brown solid 134 mg, in 55.1% yield. Mp 159–162 °C. ^{1}H NMR (300 MHz, $CDCl_3$) δ 7.22 (d, 1H, J = 7.24 Hz), 7.41–7.54 (m, 3H), 7.83 (s, 1H), 7.91 (d, 2H, J = 8.12 Hz), 8.18–8.29 (m, 4H); ^{13}C NMR (125 MHz, $CDCl_3$) δ 174.9, 168.0, 151.4, 138.8, 138.2, 134.6, 133.2, 129.8, 129.7, 129.6, 128.6, 128.3, 127.2, 126.9, 122.9, 116.8, 116.3. MS (ESI): m/z 407 $[M+H]^+$. HRMS (ESI) calcd for $C_{21}H^{13}Cl_2N_4O$ [M+H]+ 407.04676; found: 407.04689.

6.3.16. (3-(4-(5-Chloro-1*H*-benzo[*d*]imidazol-2-yl)phenyl)-5-(4-methoxyphenyl)-1,2,4-oxadiazole) 5p

This compound was prepared by method described in Section 6.3 employing ((*Z*)-4-(5-chloro-1*H*-benzo[*d*]imidazol-2-yl)-*N*′-hydroxybenzimidamide) **9c** (172 mg, 0.6 mmol), *p*-methoxy benzoic acid (76 mg, 0.5 mmol) to afford **5p** as light yellow solid 126 mg, in 52.3% yield. Mp 166–169 °C. ^{1}H NMR (300 MHz, $CDCl_3$) δ 3.87 (s, 3H), 7.12–7.24 (m, 3H), 7.54 (d, 1H, J = 7.32 Hz), 7.77 (s, 1H), 7.93 (d, 2H, J = 8.21 Hz), 8.27–8.32 (m, 4H); ^{13}C NMR (125 MHz, $CDCl_3$) δ 175.0, 167.9, 161.3, 151.2, 138.2, 134.4, 133.3, 129.6, 128.7, 128.6, 126.9, 125.6, 122.9, 118.9, 116.6, 116.2, 114.2, 56.2. MS (ESI): m/z 403 $[M+H]^+$. HRMS (ESI) calcd for $C_{22}H_{16}ClN_4O_2$ $[M+H]^+$ 403.09602; found: 403.09578.

6.3.17. (3-(4-(5-Chloro-1*H*-benzo[*d*]imidazol-2-yl)phenyl)-5-*p*-tolyl-1,2,4-oxadiazole) 5q

This compound was prepared by method described in Section 6.3 employing ((*Z*)-4-(5-chloro-1*H*-benzo[*d*]imidazol-2-yl)-*N*′-hydroxybenzimidamide) **9c** (172 mg, 0.6 mmol), *p*-tolyl benzoic acid (68 mg, 0.5 mmol) to afford **5q** as off white solid 138 mg, in 59.7% yield. Mp 179–182 °C. ^{1}H NMR (300 MHz, $CDCl_3$) δ 2.39 (s, 3H), 7.29–7.37 (m, 3H), 7.54–7.65 (m, 3H), 7.78 (s, 1H), 8.06–8.21 (m, 4H); ^{13}C NMR (125 MHz, $CDCl_3$) δ 175.1, 167.9, 151.3, 141.4, 138.3, 134.6, 133.2, 129.6, 129.3, 128.5, 128.1, 127.7, 127.2, 125.9, 122.8, 116.5, 116.4, 21.2. MS (ESI): m/z 387 $[M+H]^+$. HRMS (ESI) calcd for $C_{22}H_{16}ClN_4O$ $[M+H]^+$ 387.10118; found: 387.10109.

6.3.18. (3-(4-(5-Chloro-1*H*-benzo[*d*]imidazol-2-yl)phenyl)-5-(3,4,5-trimethoxyphenyl)-1,2,4-oxadiazole) 5r

This compound was prepared by method described in Section 6.3 employing ((*Z*)-4-(5-chloro-1*H*-benzo[*d*]imidazol-2-yl)-*N*′-hydroxybenzimidamide) **9c** (172 mg, 0.6 mmol), 3,4,5-trimethoxy benzoic acid (106 mg, 0.5 mmol) to afford **5r** as yellow solid 176 mg, in 65% yield. Mp 169–172 °C. ^{1}H NMR (300 MHz, $CDCl_3$) δ 3.89 (s, 3H), 3.93 (s, 6H), 7.16–7.25 (m, 3H), 7.57 (d, 1H, J = 7.2 Hz), 7.81 (s, 1H), 8.20–8.29 (m, 4H); ^{13}C NMR (125 MHz, $CDCl_3$) δ 174.9, 167.8, 151.2, 151.4, 143.4, 138.2, 134.3, 133.2, 129.6, 129.3, 128.3, 127.2, 122.8, 122.1, 116.6, 116.2, 106.8, 60.7, 56.3. MS (ESI): m/z 463 $[M+H]^+$. HRMS (ESI) calcd for $C_{24}H_{20}ClN_4O_4$ $[M+H]^+$ 463.11722; found: 463.11694.

6.3.19. (3-(4-(5-Methoxy-1*H*-benzo[*d*]imidazol-2-yl)phenyl)-5-phenyl-1,2,4-oxadiazole) 5s

This compound was prepared by method described in Section 6.3 employing ((*Z*)-*N*′-hydroxy-4-(5-methoxy-1*H*-benzo[*d*]imidazol-2-yl)benzimidamide) **9d** (169 mg, 0.6 mmol), benzoic acid (61 mg, 0.5 mmol) to afford **5s** as yellow solid 139 mg, in 63% yield. Mp 172–175 °C. ^{1}H NMR (300 MHz, $CDCl_3$) δ 3.88 (s, 3H), 7.12–7.23 (m, 2H), 7.32–7.51 (m, 4H), 7.79 (d, 1H, J = 7.23 Hz), 8.23–8.30 (m, 4H); ^{13}C NMR (125 MHz, $CDCl_3$) δ 175.0, 167.9, 155.7, 151.2, 138.4, 134.7, 130.1, 128.9, 128.4, 128.3, 127.1, 126.6, 114.5, 113.7, 101.9, 55.9. MS (ESI): m/z 369 $[M+H]^+$. HRMS (ESI) calcd for $C_{22}H_{17}N_4O_2$ $[M+H]^+$ 369.13507; found: 369.13534.

6.3.20. (5-(4-Fluorophenyl)-3-(4-(5-methoxy-1*H*-benzo[*d*]imidazol-2-yl)phenyl)-1,2,4-oxadiazole) 5t

This compound was prepared by method described in Section 6.3 employing ((*Z*)-*N*′-hydroxy-4-(5-methoxy-1*H*-benzo[*d*]imidazol-2-yl)benzimidamide) **9d** (169 mg, 0.6 mmol), *p*-fluoro benzoic acid (70 mg, 0.5 mmol) to afford **5t** as yellow solid 129 mg, in 55.7% yield. Mp 162–166 °C. ^{1}H NMR (300 MHz, $CDCl_3$) δ 3.85 (s, 3H), 7.04–7.21 (m, 2H), 7.57–7.62 (m, 3H), 7.71 (d, 1H, J = 7.24 Hz), 8.19–8.28 (m, 4H); ^{13}C NMR (125 MHz,

$CDCl_3$) δ 174.8, 167.9, 164.8, 155.7, 151.3, 138.4, 135.5, 134.7, 130.2, 128.4, 128.2, 127.3, 124.0, 115.9, 114.5, 113.6, 101.8, 56.0. MS (ESI): *m/z* 387[M+H]$^+$. HRMS (ESI) calcd for $C_{22}H_{16}FN_4O_2$ [M+H]$^+$ 387.12557; found: 387.12516.

6.3.21. (5-(4-Chlorophenyl)-3-(4-(5-methoxy-1*H*-benzo[*d*]imidazol-2-yl)phenyl)-1,2,4-oxadiazole) 5u

This compound was prepared by method described in Section 6.3 employing ((*Z*)-*N*′-hydroxy-4-(5-methoxy-1*H*-benzo[*d*]imidazol-2-yl)benzimidamide) **9d** (169 mg, 0.6 mmol), *p*-chloro benzoic acid (78 mg, 0.5 mmol) to afford **5u** as yellow solid 119 mg, in 49% yield. Mp 192–196 °C. ^{1}H NMR (500 MHz, $CDCl_3$) δ 3.83 (s, 3H), 7.02 (d, 1H, *J* = 7.21 Hz), 7.21 (s, 1H), 7.54 (d, 2H, *J* = 8.11 Hz), 7.59 (d, 1H, *J* = 7.24 Hz), 7.83 (d, 2H, *J* = 8.12 Hz), 8.21–8.32 (dd, 4H, *J* = 8.3, 5.62 Hz); ^{13}C NMR (125 MHz, $CDCl_3$) δ 174.9, 168.0, 155.6, 151.4, 139.8, 138.6, 135.6, 134.5, 129.9, 129.7, 128.3, 128.6, 127.3, 126.8, 114.4, 113.6, 101.8, 55.9. MS (ESI): *m/z* 403 [M+H]$^+$. HRMS (ESI) calcd for $C_{22}H_{16}ClN_4O_2$ [M+H]$^+$ 403.09603; found: 403.09576.

6.3.22. (3-(4-(5-Methoxy-1*H*-benzo[*d*]imidazol-2-yl)phenyl)-5-(4-methoxyphenyl)-1,2,4-oxadiazole) 5v

This compound was prepared by method described in Section 6.3 employing ((*Z*)-*N*′-hydroxy-4-(5-methoxy-1*H*-benzo[*d*]imidazol-2-yl)benzimidamide) **9d** (169 mg, 0.6 mmol), *p*-methoxy benzoic acid (76 mg, 0.5 mmol) to afford **5v** as pale yellow solid 125 mg, in 52.4% yield. Mp 179–182 °C. ^{1}H NMR (300 MHz, $CDCl_3$) δ 3.87 (s, 3H), 3.89 (s, 3H), 6.91 (d, 1H, *J* = 7.24 Hz), 7.15 (s, 1H), 7.46–7.52 (m, 2H), 7.57 (d, 1H, *J* = 7.26 Hz), 7.89–8.12 (m, 2H), 8.27–8.32 (m, 4H); ^{13}C NMR (125 MHz, $CDCl_3$) δ 174.8, 167.9, 161.4, 155.6, 151.2, 138.6, 135.4, 134.6, 128.7, 128.5, 126.9, 125.5, 118.9, 118.8, 114.4, 114.3, 113.7, 101.9, 56.3. MS (ESI): *m/z* 399 [M+H]$^+$. HRMS (ESI) calcd for $C_{23}H_{19}N_4O_3$ [M+H]$^+$ 399.14565; found: 399.14559.

6.3.23. (3-(4-(5-Methoxy-1*H*-benzo[*d*]imidazol-2-yl)phenyl)-5-*p*-tolyl-1,2,4-oxadiazole) 5w

This compound was prepared by method described in Section 6.3 employing ((*Z*)-*N*′-hydroxy-4-(5-methoxy-1*H*-benzo[*d*]imidazol-2-yl)benzimidamide) **9d** (169 mg, 0.6 mmol), *p*-tolyl benzoic acid (68 mg, 0.5 mmol) to afford **5w** as yellow solid 137 mg, in 57.6% yield. Mp 184–187 °C. ^{1}H NMR (300 MHz, $CDCl_3$) δ 2.36 (s, 3H), 3.78 (s, 3H), 6.99 (d, 1H, *J* = 8.26 Hz), 7.18 (s, 1H), 7.32–7.46 (m, 4H), 7.61 (d, 1H, *J* = 8.23 Hz), 8.21–8.31 (m, 4H); ^{13}C NMR (125 MHz, $CDCl_3$) δ 175.1, 167.9, 155.5, 151.3, 141.3, 138.5, 135.4, 134.6, 129.4, 128.5, 128.4, 127.7, 127.2, 125.8, 114.6, 113.7, 101.7, 56.2, 21.3. MS (ESI): *m/z* 383 [M+H]$^+$. HRMS (ESI) calcd for $C_{23}H_{19}N_4O_2$ [M+H]$^+$ 383.15046; found: 383.15032.

6.3.24. (3-(4-(5-Methoxy-1*H*-benzo[*d*]imidazol-2-yl)phenyl)-5-(3,4,5-trimethoxyphenyl)-1,2,4-oxadiazole) 5x

This compound was prepared by method described in Section 6.3 employing ((*Z*)-*N*′-hydroxy-4-(5-methoxy-1*H*-benzo[*d*]imidazol-2-yl)benzimidamide) **9d** (169 mg, 0.6 mmol), 3,4,5-trimethoxy benzoic acid (106 mg, 0.5 mmol) to afford **5x** as yellow solid 157 mg, in 57.2% yield. Mp 187–189 °C. ^{1}H NMR (500 MHz, $CDCl_3$) δ 3.86 (s, 3H), 3.90 (s, 3H), 3.99 (s, 6H), 6.84 (d, 1H, *J* = 8.68 Hz), 7.12 (s, 1H), 7.42 (s, 2H), 7.50 (d, 1H, *J* = 8.68 Hz), 8.30 (dd, 4H, *J* = 8.30, 7.93 Hz); ^{13}C NMR (125 MHz, $CDCl_3$) δ 174.9, 167.7, 155.5, 151.9, 151.3, 143.3, 138.6, 135.5, 134.4, 129.3, 128.4, 127.1, 122.2, 114.5, 113.7, 106.9, 101.9, 56.4, 60.8. MS (ESI): *m/z* 459 [M+H]$^+$. HRMS (ESI) calcd for $C_{25}H_{23}N_4O_5$ [M+H]$^+$ 459.16665; found: 459.16643.

7. Biology

7.1. In vitro anti proliferative activity (SRB assay)

The compounds were evaluated for their in vitro anti-proliferative activity at National Cancer Institute (NCI), USA against full NCI 60 cell lines panel representing on full nine human systems as leukemia, melanoma and cancers of lung, colon, brain, breast, ovary, kidney and prostate in accordance with their applied protocol (used SRB assay). The screening, begins with the evaluation of the compounds against the 60 cell lines at one dose of 10 mM. The single dose screen results were reported as a mean graph. Compounds that exhibited significant growth inhibition in single dose screening were further evaluated against the 60 cell panel at five concentration levels. The human tumor cell lines of the screening panel were grown in RPMI 1640 medium containing 5% fetal bovine serum and 2 mM L-glutamine. For a typical screening experiment, cells seeded into 96 well microtiter plates in 100 μL at plating densities ranging from 5000 to 40,000 cells/well depending on the doubling time of individual cell lines. After cell seeding, the plates incubated at 37 °C, 5% CO_2, 95% air and 100% relative humidity for 24 h prior to addition of experimental drugs. After 24 h, two plates of each cell line fixed in situ with TCA, to represent a measurement of the cell population for each cell line at the time of drug addition (Tz). Test compounds solubilized in dimethyl sulfoxide at 400-fold the desired final maximum test concentration and stored frozen prior to use. At the time of drug addition, an aliquot of frozen concentrate was thawed and diluted to twice the desired final maximum test concentration with complete medium containing 50 mg/mL gentamicin. Additional four, 10-fold or log serial dilutions are made to provide a total of five drug concentrations plus control. Aliquots of 100 μL of these different drug dilutions added to the appropriate microtiter wells already containing 100 μL of medium, resulting in the required final drug concentrations. Following drug addition, the plates were incubated for an additional 48 h at 37 °C, 5% CO_2, 95% air, and 100% relative humidity. For adherent cells, the assay terminated by the addition of cold TCA. Cells fixed in situ by the addition of 50 μL of cold 50% (w/v) TCA (final concentration, 10% TCA) and incubated for 60 min at 4 °C. The supernatant was discarded, and the plates washed five times with tap water and then air dried. Then, 0.4% (w/v) solution of Sulforhodamine B (SRB) in 1% acetic acid, (100 μL) was added to each well and plates incubated for 10 min at room temperature. Unbound dye removed by washing five times with 1% acetic acid and then the plates air dried. Bound stain solubilized with 10 mM trizma base and the absorbance was recorded on an automated plate reader at a wavelength of 515 nm. For Non adherent cells, the methodology was same except that the assay terminated by fixing settled cells at the bottom of the wells by adding 50 μL of 80% TCA (final concentration, 16% TCA). Using the seven absorbance measurements [time zero, (Tz), control growth, (C) and test growth in the presence of drug at the five concentration levels (Ti)], the percentage growth was calculated at each of the test concentrations levels using the following formula:

$$(Ti - Tz)/(C - Tz) \times 100 \text{ for concentrations for which } Ti > / = Tz$$

$$(Ti - Tz)/Tz \times 100 \text{ for concentrations for which } Ti < Tz.$$

Three dose response parameters (GI_{50}, TGI and LC_{50}) were calculated for each experimental agent. Growth inhibition of 50% (GI_{50}) calculated from $[(Ti - Tz)/(C - Tz)] \times 100 = 50$, which was the drug concentration resulting in a 50% reduction in the net protein increase (as measured by SRB staining) in control cells during the drug incubation. The drug concentration resulting in total growth inhibition (TGI) calculated from Ti = Tz. The LC_{50}

(concentration of drug resulting in a 50% reduction in the measured protein at the end of the drug treatment as compared to that at the beginning) indicating a net loss of cells following treatment was calculated from $[(Ti - Tz)/Tz] \times 100 = -50$. Values were calculated for each of these three parameters, if the level of activity was reached; however, if the effect is not reached or was exceeded, the value for that parameter expressed as greater or less than the maximum or minimum concentration tested.

7.2. Cell cycle analysis

MCF-7 cells (1×10^6 cells/well) were seeded in six well plates and treated with compounds **5l**, **5x** and Nocodazole at concentrations of 1 μM and 3 μM for 48 h. After the treatment, both floating and trypsinised adherent cells were collected, washed with PBS and fixed with 70% ethanol. After fixation cells were washed with PBS and stained with 50 μg/mL propidium iodide in hypotonic lysis buffer (0.1% sodium citrate, 0.1% Triton X-100) containing DNase-free RNase-A for 20 min. Stained cells were analyzed using fluorescence-activated cell sorter caliber (Becton Dickinson).

7.3. In vitro tubulin polymerization

A fluorescence based in vitro tubulin polymerization assay was performed according to the manufacturer's protocol (BK011, Cytoskeleton, Inc.). Briefly, the reaction mixture in a total volume of 10 μL contained PEM buffer, GTP (1 μM) in the presence or absence of test compounds **5l**, **5x** and nocodazole (final concentration of 3 μM). Tubulin polymerization was followed by a time dependent increase in fluorescence due to the incorporation of a fluorescence reporter into microtubules as polymerization proceeds. Fluorescence emission at 420 nm (excitation wavelength is 360 nm) was measured by using a Varioscan multimode plate reader (Thermo scientific Inc.). The IC_{50} value was defined as the drug concentration required to inhibit 50% of tubulin assembly compared to control. The reaction mixture for these experiments include: tubulin (3 mg/mL) in PEM buffer, GTP (1 mM), in the presence or absence of test compounds at various concentrations. Polymerization was monitored by increase in the fluorescence as mentioned above at 37 °C.

7.4. Immunohistochemistry of tubulin

MCF-7 cells were seeded on glass cover slips, incubated for 48 h in the presence or absence of test compounds **5l**, **5x** and nocodazole at a concentration of 1 μM. Following the termination of incubation, cells were fixed with 3% formaldehyde, 0.02% glutaraldehyde in PBS and permeabilized by dipping the cells in 100% methanol (−20 °C). Later, cover slips were blocked with 1% BSA in phosphate buffered saline for 1 h followed by incubation with a primary antitubulin (mouse monoclonal) antibody and FITC conjugated secondary mouse anti IgG antibody. Photographs were taken using the confocal microscope, equipped with FITC settings and the pictures were analyzed for the integrity of microtubule network.

7.5. Colchicine competitive binding assay

The test compounds **5l**, **5x**, nocodazole and taxol of various concentrations 0, 5, 10 and 15 μM were co-incubated with 4 μM colchicine in 30 mM Tris buffer containing 3 μM tubulin for 60 min at 37 °C. Nocodazole was used as a positive control whereas taxol was used as negative control which does not bind at colchicine site. After incubation the fluorescence of tubulin–colchicine complex was determined by using Tecan multimode reader at excitation wavelength at 350 nm and emission wavelength at 435 nm. 30 mM Tris buffer was used as blank which was subtracted from all the samples. The experiment was carried out both in the presence and absence of colchicine to obtain fluorescence values of the desired tubulin–colchicine complex. The fluorescence values of tubulin–conjugates complex was subtracted from the tubulin-conjugates-colchicine complex. Fluorescence values are normalized to DMSO control.

7.6. Hoechst staining

MCF-7 cells were seeded at a density of 10,000 cells over 18-mm coverslips and incubated for 24 h. Then, the medium was replaced, and cells were treated with 1 μM concentration of compounds **5l**, **5x** and nocodazole for 24 h. Cells treated with vehicle (0.001% DMSO) were included as controls for all experiments. Cells were fixed with 4% paraformaldehyde and stained with solution of Hoechst 33342 (Sigma Aldrich) 5 μg/mL in PBS. After incubation for 30 min at 37 °C, excess dye was washed with PBS and cells from each dish were captured from randomly selected fields under fluorescent microscope (Leica, Germany) to qualitatively determine the proportion of viable and apoptotic cells based on their relative fluorescence and nuclear fragmentation.

7.7. Mitochondrial membrane potential

MCF-7 (1×10^6 cells/well) cells were cultured in six-well plates and treated with compounds **5l** and **5x** at 1 μM concentration for 24 h. After treatment, cells were collected by trypsinization and washed with PBS followed by suspending in 5,5′,6,6′-tetrachloro-1,1′,3,3′-tetraethyl-imidacarbocyanine iodide (JC-1 dye) solution (10 mM/L) and incubated at 37 °C for 15 min. Cells were rinsed three times with medium and suspended in pre warmed medium. The cells were then subjected fluorescence-activated cell sorter caliber (Becton Dickinson) in the FL1, FL2 channel to detect mitochondrial potential

7.8. DNA fragmentation

MCF-7 cells were seeded (1×10^6) in six well plates and allowed to adhere for 24 h. Cells were treated with compounds **5l** and **5x** at 2 μM concentration fore 24 h. Cells were collected and centrifuged at 2500 rpm for 5 min at 4 °C. Pellet was collected and washed with PBS, added 250 μL of lysis buffer (100 mM NaCl, 5 mM EDTA, 10 mM Tris HCl pH 8.0, 0.25% SDS) containing 400 μg/mL DNase free RNase A and incubated at 37 °C for 90 min followed by incubation with proteinase K (200 μg/mL) at 50 °C for 1 h. Centrifuged at 3000 rpm for 5 min at 4 °C and collected supernatant. Then added 65 μL of 10 M Ammonium acetate and 500 μL of ice cold ethanol and mixed well. And these samples were incubated at −80 °C for 1 h. After incubation samples were centrifuged at 12,000 rpm for 20 min at 4 °C. After centrifuge, pellet was washed with 80% ethanol and air dried for 10 min at room temperature. Dissolved the pellet in 50 μL of TE buffer and DNA laddering was determined by using 2% agarose gel electrophoresis in TE Buffer.

7.9. Annexin V-FITC assay

MCF-7 cells (1×10^6) were seeded in six-well plates and allowed to adhere overnight. The medium was then replaced with medium containing 1 μM concentrations of compounds **5l** and **5x** and incubated for 24 h. Cells treated with DMSO (0.001%) was used as control. After 24 h of drug treatment, cells were harvested, washed with PBS. Then the cells (1×10^6) were stained with Annexin V-FITC and propidium iodide using the Annexin-V-PI apoptosis detection kit (Sigma Aldrich-India). Flow cytometry

was performed using a FACScan (Becton Dickinson) equipped with a single 488 nm argon laser. Annexin V-FITC was analyzed using excitation and emission settings of 488 nm and 535 nm (FL-1 channel); PI, 488 nm and 610 nm (FL-2 channel). Debris and clumps were gated out using forward and orthogonal light scatter.

7.10. Molecular modeling procedure

All the geometries were optimized in Gaussian 09 using PM3 semi-empirical method.[27] Protein structure was downloaded from Protein Data Bank (PDB ID: 3E22).[28] Docking studies were performed using AutoDock 4.2 software.[29] The analysis of intermolecular interactions has been performed using Pymol, v. 0.99.[30]

Acknowledgements

T.S.R., V.K.N. thanks NIPER, Hyderabad, India for the award of research fellowship and A.V.S.R., V.S. thanks CSIR, New Delhi for the award of the senior research fellowships. We also thank CSIR for financial support under the 12th Five Year plan project 'Affordable Cancer Therapeutics' (CSC0301) and 'Small Molecules in Lead Exploration (SMiLE)' (CSC0111).

References and notes

1. El-Nezhawy, A. O. H.; Biuomy, A. R.; Hassan, F. S.; Ismaiel, A. K.; Omar, H. A. *Bioorg. Med. Chem.* **2013**, *21*, 1661.
2. (a) Fang, B.; Zhou, C.; Rao, X. *Eur. J. Med. Chem.* **2010**, *45*, 4388; (b) Ranjith, P. K.; Rajeesh, P.; Haridas, K. R.; Susanta, N. K. *Bioorg. Med. Chem. Lett.* **2013**, *23*, 5228.
3. Kus, C.; Ayhan-Kılcıgil, G.; Ozbey, S.; Betu, F.; Kaynak, I.; Kaya, M.; Coban, T.; Can-Eke, B. *Bioorg. Med. Chem.* **2008**, *16*, 4294.
4. (a) Miller, J. F.; Turner, E. M.; Gudmundsson, K. S.; Jenkinson, S.; Splatenstein, A.; Thomson, M.; Wheelan, P. *Bioorg. Med. Chem. Lett.* **2010**, *20*, 2125; (b) Monforte, A.; Logoteta, P.; Luca, L. D.; Iraci, N.; Ferro, S.; Maga, G.; Clercq, E. D.; Pannecouque, C.; Chimirri, A. *Bioorg. Med. Chem.* **2010**, *18*, 1702.
5. (a) Achar, K. C. S.; Hosamani, K. M.; Seetharamareddy, H. R. *Eur. J. Med. Chem.* **2010**, *45*, 2048; (b) Chen, G.; Liu, Z.; Zhang, Y.; Shan, X.; Jiang, L.; Zhao, Y.; He, W.; Feng, Z.; Yang, S.; Liang, G. *ACS Med. Chem. Lett.* **2013**, *4*, 69.
6. (a) Omar, M. A.; Shaker, Y. M.; Galal, S. A.; Ali, M. M.; Kerwin, S. M.; Li, J.; Tokuda, H.; Ramadan, R. A.; El Diwani, H. I. *Bioorg. Med. Chem.* **2012**, *20*, 6989; (b) Wang, T.; Sepulveda, M.; Gonzales, P.; Gately, S. *Bioorg. Med. Chem. Lett.* **2013**, *23*, 4790; (c) Rashedy, Ahmed A.; El, Hassan Y. *Drug Ther.* **2013**, *8*, 1.
7. (a) Singh, M. P.; Joseph, T.; Kumar, S.; Bathini, Y.; Lown, J. W. *Chem. Res. Toxicol.* **1992**, *5*, 597; (b) Jenkins, T. C. *Curr. Med. Chem.* **2000**, *7*, 99.
8. (a) Duanmu, C.; Shahrik, L. K.; Holly, H. H.; Hamel, E. *Cancer Res.* **1989**, *49*, 1344; (b) Vasquez, R. J.; Howell, B.; Yvon, A. M.; Wadsworth, P.; Cassimeris, L. *Mol. Biol. Cell* **1997**, *8*, 973.
9. (a) Lissitchkov, T.; Arnaudov, D.; Peytchev, D.; Merkle, K. *J. Cancer Res. Clin. Oncol.* **2006**, *132*, 99; (b) Knauf, W. U.; Lissichkov, T.; Aldaoud, A. *J. Clin. Oncol.* **2009**, *27*, 4378.
10. Kamal, A.; Reddy, M. K.; Shaik, T. B.; Srikanth, Y. V. V.; Reddy, V. S.; Kumar, G. B.; Kalivendi, S. V. *Eur. J. Med. Chem.* **2012**, *50*, 9.
11. (a) White, A. W.; Almassy, R.; Calvert, A. H.; Curtin, N. J.; Griffin, R. J.; Hostomsky, Z.; Newell, D. R.; Srinivasan, S.; Golden, B. T. *J. Med. Chem.* **2000**, *43*, 4084; (b) Griffin, R. J.; Srinivasan, S.; Bowman, K.; Calvert, A. H.; Curtin, N. J.; Newell, D. R.; Pemberton, L. C.; Golding, B. T. *J. Med. Chem.* **1998**, *41*, 5247.
12. (a) Li, Y. Q.; Tan, C. Y.; Gao, C. M.; Zhang, C. L.; Luan, X. D.; Chen, X. W.; Liu, H. X.; Chen, Y. Z.; Jiang, Y. Y. *Bioorg. Med. Chem.* **2011**, *19*, 4529; (b) Singh, M.; Tandon, V. *Eur. J. Med. Chem.* **2011**, *46*, 659.
13. Barreca, M. L.; Rao, A.; Luca, L. D.; Zappala, M.; Monforte, A. M. *J. Med. Chem.* **2005**, *48*, 3433.
14. Nicolaides, D. N.; Fylaktakidou, K. C.; Litinas, K. E.; Hadjipavlou-Litina, D. *Eur. J. Med. Chem.* **1998**, *33*, 715.
15. (a) Khatik, G. L.; Kaur, J.; Kumar, V.; Tikoo, K.; Nair, V. A. *Bioorg. Med. Chem.* **2003**, *11*, 1821.
16. (a) Kumar, D.; Patel, G.; Chavers, A. K.; Chang, K. H.; Shah, K. *Eur. J. Med. Chem.* **2011**, *46*, 3085; (b) Bora, O.; Rajesh, D.; Bashir; Pradhan, Vidya; Farooqui, Mazahar *Mini Rev. Med. Chem.* **2014**, *14*, 355; (c) Rashid, M.; Husain, A.; Mishra, R. *Eur. J. Med. Chem.* **2012**, *54*, 855.
17. (a) Luthman, K.; Borg, S.; Hacksell, U. *Methods Mol. Med.* **1999**, *23*, 1; (b) Hamzé, A.; Hernandez, J. F.; Fulcrand, P.; Martinez, J. *J. Org. Chem.* **2003**, *68*, 7316.
18. (a) Zhang, H. Z.; Kasibhatla, S.; Kuemmerle, J.; Kemnitzer, W.; Ollis-Mason, K.; Qiu, L.; Crogan-Grundy, C.; Tseng, B.; Drewe, J.; Cai, S. X. *J. Med. Chem.* **2005**, *48*, 5215; (b) Kumar, D.; Patel, G.; Johnson, E. O.; Shah, K. *Bioorg. Med. Chem. Lett.* **2009**, *19*, 2739; (c) dos Anjos, J. V. *Eur. J. Med. Chem.* **2009**, *44*, 3571; (d) Jessen, K. A.; English, N. M.; Wang, J. Y.; Maliartchouk, S.; Archer, S. P.; Qiu, L.; Brand, R.; Kuemmerle, J.; Zhang, H. Z.; Gehlsen, K.; Drewe, J.; Tseng, B.; Cai, S. X.; Kasibhatla, S. *Mol. Cancer Ther.* **2005**, *4*, 761.
19. (a) Rashid, M.; Husain, A.; Siddiqui, A. A.; Mishra, R. *Eur. J. Med. Chem.* **2013**, *62*, 785; (b) Kiselyov, A. S.; Semenova, M. N.; Chernyshova, N. B.; Leitao, A.; Samet, A. V.; Kislyi, K. A.; Raihstat, M. M.; Oprea, T.; Lemcke, H.; Lantow, M.; Weiss, D. G.; Ikizalp, N. N.; Kuznetsov, S. A.; Semenov, V. V. *Eur. J. Med. Chem.* **2010**, *45*, 1683.
20. Wignall, S. M.; Gray, N. S.; Chang, Y. T.; Juarez, L.; Jacob, R.; Burlingame, A.; Schultz, P. G.; Heald, R. *Chem. Biol.* **2004**, *11*, 135.
21. Bhalla, K. N. *Oncogene* **2003**, *22*, 9075.
22. Liu, Z.; Zhou, Z.; Tian, W.; Fan, X.; Xue, D.; Yu, L.; Yu, Q.; Long, Y.-Q. *Chem. Med. Chem.* **2012**, *7*, 680.
23. Mollinedo, F.; Gajate, C. *Apoptosis* **2003**, *8*, 413.
24. Green, D. R.; Reed, J. C. *Science* **1998**, *281*, 1309.
25. Hou, Q.; Zhao, T. B.; Zhang, H. L.; Lu, H. X.; Zhang, Q. X.; Sun, L.; Fan, Z. *Mol. Immunol.* **2008**, *45*, 1044.
26. Zhu, H.; Zhang, J.; Xue, N.; Hu, Y.; Yang, B.; He, Q. *Invest. New Drugs* **2010**, *28*, 493.
27. Frisch, M. J.; Trucks, G. W.; Schlegel, H. B.; Scuseria, G. E.; Robb, M. A.; Cheeseman, J. R.; Scalmani, G.; Barone, V.; Mennucci, B.; Petersson, G. A.; Nakatsuji, H.; Caricato, M.; Li, X.; Hratchian, H. P.; Izmaylov, A. F.; Bloino, J.; Zheng, G.; Sonnenberg, J. L.; Hada, M.; Ehara, M.; Toyota, K.; Fukuda, R.; Hasegawa, J.; Ishida, M.; Nakajima, T.; Honda, Y.; Kitao, O.; Nakai, H.; Vreven, T.; Montgomery, J. A.; Peralta, J. E.; Ogliaro, F.; Bearpark, M.; Heyd, J. J.; Brothers, E.; Kudin, K. N.; Staroverov, V. N.; Kobayashi, R.; Normand, J.; Raghavachari, K.; Rendell, A.; Burant, J. C.; Iyengar, S. S.; Tomasi, J.; Cossi, M.; Rega, N.; Millam, J. M.; Klene, M.; Knox, J. E.; Cross, J. B.; Bakken, V.; Adamo, C.; Jaramillo, J.; Gomperts, R.; Stratmann, R. E.; Yazyev, O.; Austin, A. J.; Cammi, R.; Pomelli, C.; Ochterski, J. W.; Martin, R. L.; Morokuma; Zakrzewski; Voth, G. A.; Salvador, P.; Dannenberg, J. J.; Dapprich, S.; Daniels, A. D.; Farkas; Foresman, J. B.; Ortiz, J. V.; Cioslowski, J.; Fox, D. J. *Gaussian 09 (Revision B.1)*; Gaussian: Wallingford, CT, 2010.
28. Cormier, A.; Marchand, M.; Ravelli, R. B. G.; Knossow, M.; Gigant, B. *EMBO Rep.* **2008**, *9*, 1101.
29. Morris, G. M.; Huey, R.; Lindstrom, W.; Sanner, M. F.; Belew, R. F.; Goodsell, D. S.; Olson, A. J. *J. Comput. Chem.* **2009**, *16*, 2785.
30. The PyMOL Molecular Graphics System, Version 0.99, Schrçdinger, LLC; http://www.pymol.org/.
31. Singhal, N.; Johar, M.; Lown, J. W.; Sondhi, S. M. *Sulfur Silicon Relat. Elem.* **2001**, *174*, 81.